Lung Precancer Analysis

Jaewoong Lee   S. Park   Y. Choi   I. Yun   Semin Lee

Department of Biomedical Engineering
Ulsan National Institute of Science and Technology

jwlee230@unist.ac.kr

2022-01-17

Overview

1. Introduction

1. Introduction

1.1. Lung Cancer

Lung Cancer?

The most common cancer

12.3 % of all cancers (Minna, Roth, & Gazdar, 2002)

The most important factor

Tobacco

Cancer Survival Rate in Korea

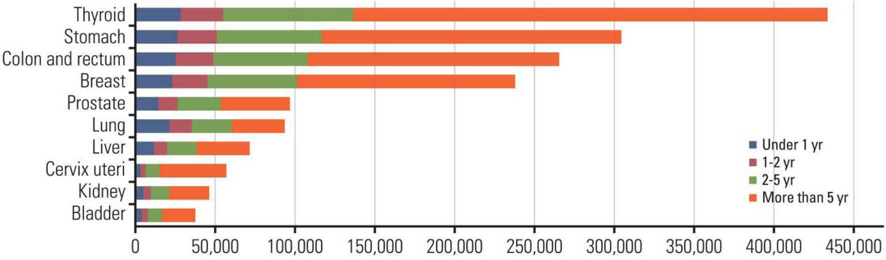

Figure: Common cancer survival rates (S. Hong et al., 2021)

Survival rate (More than 5 year)

- Tyroid: 68.4 %
- Lung: 35.4 %

Type of Lung Cancer I

Types of lung cancer (Collins, Haines, Perkel, & Enck, 2007):

1. Adenocarcinoma (LUAD) (40 %) ★
2. Squamous cell carcinoma (LUSC) (25 %) ★
3. Small cell carcinoma (20 %)
4. Large cell carcinoma (10 %)
5. Adenosquamous carcinoma ($<$ 5 %)
6. Carcinoid ($<$ 5 %)
7. Bronchioalveolar (Bronchial gland carcinoma)
8. ...

Type of Lung Cancer II

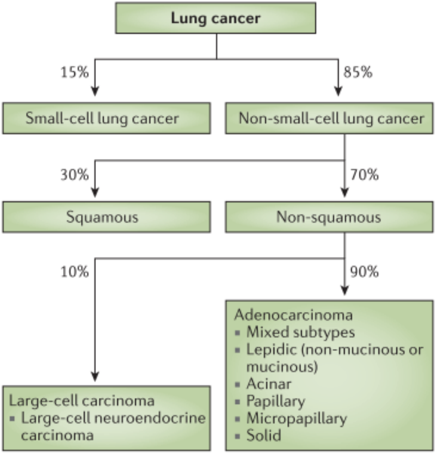

Figure: Lung cancer classification (Gridelli et al., 2015)

1. Introduction

1.2. Non-small cell lung cancer

Non-small cell lung cancer (NSCLC)

Types of NSCLC (Goldstraw et al., 2011):

- Adenocarcinoma (ICDO 8140/3)
- Squamous cell carcinoma (ICDO 8070/3)
- Large-cell carcinoma (ICDO 8012/3)
- ...

1. Introduction

1.3. LUAD

LUAD

TCGA LUAD (Duhig et al., 2014)

- 81 % patients reported past/present tobacco smoking.
- Candidate driver genes: RTK, RAS, and RAF (38 %)
- Cancer-associated mutations: KRAS (32 %), EGFR (11 %), and BRAF (7 %)
- Enriched mutations: TP53, KEAP1, NF1, and RIT1 ($p < 0.01$)
- Fusions: ROS1 and RET

1. Introduction

1.4. LUSC

LUSC

TCGA LUSC (Dosenbach et al., 2007)

- 96 % patients reported past/present tobacco smoking.
- Not present EGFR and ALK fusions.
- Recurrent mutations: TP53, NFE2L2, KEAP1, BAI3, FBXW7, GRM8, MUC16, RUNX1T1, STK11, and ERBB4
- High rate of copy number alteration compared with other TCGA projects.
- Amplication of NFE2L2, MYC, CDK6, MDM2, BCL2L1, and EYS.
- Deletion of FOXP1, PTEN, and NF1

1. Introduction

1.5. LUAD vs. LUSC

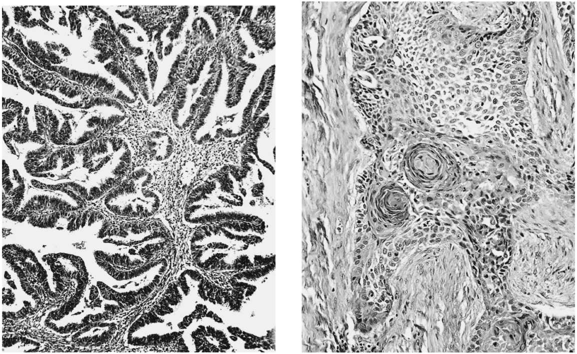

(a) LUAD

(b) LUSC

Figure: LUAD and LUSC histology in Lung cancer (Travis, 2002)

LUAD vs. LUSC II

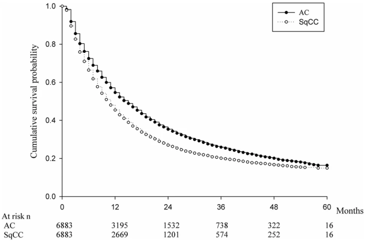

(a) All patients

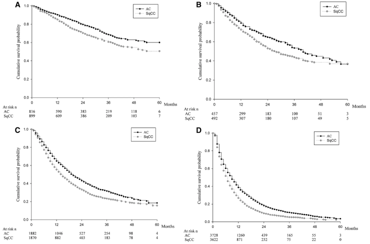

(b) By cancer stages

Figure: Kaplan-Meiere survival curves for LUAD & LUSC (B.-Y. Wang et al., 2020)

Findings

LUSC is more dangerous than LUAD. $\because p < 0.001$

1. Introduction

1.6. Study Objectives

Study Objectives

Find different mutations

- between WES vs. WTS
- from cancer vs. precancer

Ultra-deep sequencing

to find an *infinitesimal* quantity of Non-Circulating Tumor DNA

- from blood
- from urine
- from bronchus

2. Materials

Lung Cancer Data

- Exome (WES) (sample n=289) + Transcriptome (WTS) (sample n=166)
- Normal + {AAH, CIS + AIS, Dysplasia, MIA} + Primary
  - Adenocarcinoma in situ
  - Atypical adenomatous hyperplasia
  - Carcinoma *in situ*
  - Dysplasia
  - Minimally invasive adenocarcinoma
- Adenocarcinoma (LUAD) & Squamouse cell carcinoma (LUSC)
  1. Normal → AAH → AIS → MIA → LUAD (patient n=28)
  2. Normal → Dysplasia → CIS → LUSC (patient n=80)

2. Materials

2.1. WES Data

WES Data Composition

Table: Number of WES samples

Cancer Subtype	Stage	Number of Samples
LUSC	Normal	77
	Dysplasia	5
	AAH	8
	CIS+AIS	73
	Primary	77
	Total	240
LUAD	Normal	18
	AAH	15
	CIS+AIS	9
	MIA	1
	Primary	18
	Total	61

WES Data Composition with Recurrence I

Table: LUSC WES Data with Recurrence

Recurrence?	Stage	Number of Samples
Recurrence	Normal	14
	Dysplasia	4
	CIS+AIS	12
	Primary	14
	Total	44
Non-recurrence	Normal	63
	Dysplasia	1
	AAH	8
	CIS+AIS	61
	Primary	63
	Total	196

WES Data Composition with Recurrence II

Table: LUAD WES Data with Recurrence

Recurrence?	Stage	Number of Samples
Recurrence	Normal	5
	AAH	8
	CIS+AIS	2
	Primary	5
	Total	20
Non-recurrence	Normal	13
	AAH	7
	CIS+AIS	7
	MIA	1
	Primary	13
	Total	41

WES Data Composition with Smoking I

Table: LUSC WES Data with Smoking

Smoking?	Stage	Number of Samples
Never	Normal	3
	CIS+AIS	3
	Primary	3
	Total	9
Ex	Normal	41
	Dysplasia	1
	AAH	4
	CIS+AIS	40
	Primary	41
	Total	127
Current	Normal	33
	Dysplasia	4
	AAH	4
	CIS+AIS	30
	Primary	33
	Total	104

WES Data Composition with Smoking II

Table: LUAD WES Data with Smoking

Smoking?	Stage	Number of Samples
Never	Normal	1
	CIS+AIS	1
	Primary	1
	Total	3
Ex	Normal	10
	AAH	9
	CIS+AIS	6
	Primary	10
	Total	35
Current	Normal	7
	AAH	6
	CIS+AIS	2
	MIA	1
	Primary	7
	Total	23

2. Materials

2.2. WTS Data

WTS Data Composition

Table: Number of WTS samples

Cancer Subtype	Stage	Number of Samples
LUSC	Normal	17
	Dysplasia	2
	CIS+AIS	34
	Primary	36
	Total	89
LUAD	Normal	13
	AAH	1
	CIS+AIS	5
	Primary	6
	Total	25

WTS Data Composition with Recurrence I

Table: LUSC WTS Data with Recurrence

Recurrence?	Stage	Number of Samples
Recurrence	Normal	1
	Dysplasia	1
	CIS+AIS	5
	Primary	6
	Total	13
Non-recurrence	Normal	16
	Dysplasia	1
	CIS+AIS	29
	Primary	30
	Total	76

WTS Data Composition with Recurrence II

Table: LUAD WTS Data with Recurrence

Recurrence?	Stage	Number of Samples
Recurrence	Normal	2
	CIS+AIS	1
	Primary	1
	Total	4
Non-recurrence	Normal	11
	AAH	1
	CIS+AIS	4
	Primary	5
	Total	21

WTS Data Composition with Smoking I

Table: LUSC WTS Data with Smoking

Smoking?	Stage	Number of Samples
Never	Normal	1
	CIS+AIS	1
	Primary	2
	Total	4
Ex	Normal	8
	Dysplasia	1
	CIS+AIS	21
	Primary	22
	Total	52
Current	Normal	8
	Dysplasia	1
	CIS+AIS	12
	Primary	12
	Total	33

WTS Data Composition with Smoking II

Table: LUAD WTS Data with Smoking

Smoking?	Stage	Number of Samples
Never	Normal	10
	AAH	1
	CIS+AIS	3
	Primary	4
	Total	18
Ex	Normal	3
	CIS+AIS	1
	Primary	1
	Total	5
Current	CIS+AIS	1
	Primary	1
	Total	2

3. Methods

3. Methods

3.1. Workflows

Data pre-processing for variant discovery

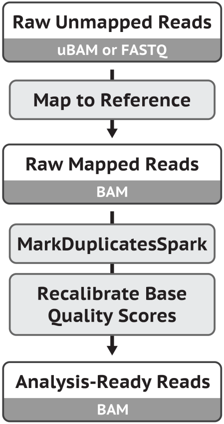

Figure: Data pre-processing for variant discovery (Van der Auwera et al., 2013; DePristo et al., 2011)

Somatic short variant discovery

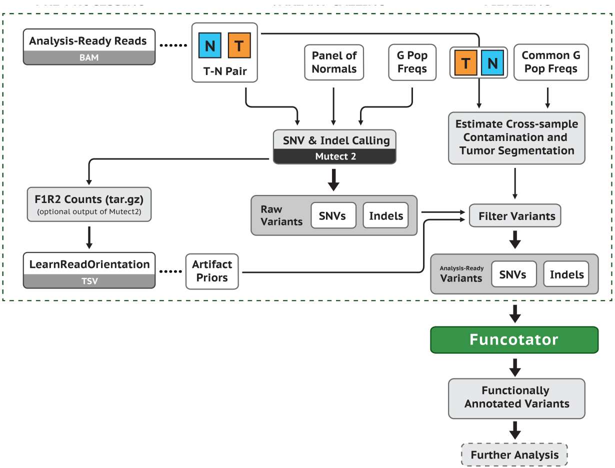

Figure: Somatic short variant (SNVs + Indels) discovery workflow (Van der Auwera et al., 2013; DePristo et al., 2011)

Germline short variant discovery

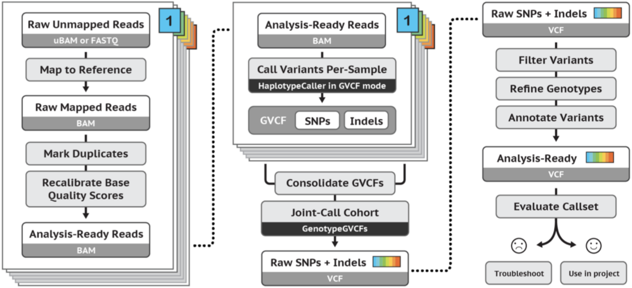

Figure: Germline short variant (SNVs + Indels) discovery workflow (Van der Auwera et al., 2013; DePristo et al., 2011)

RNA-seq short variant discovery

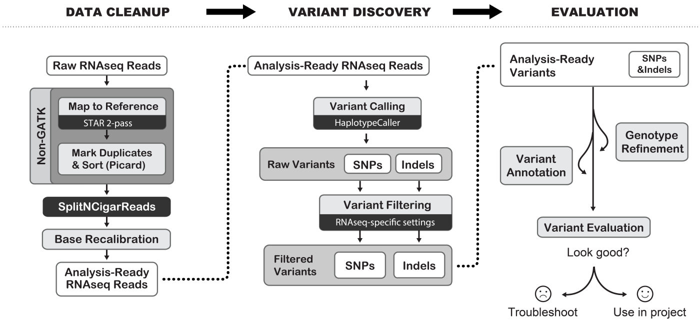

Figure: RNA-seq short variant (SNVs + Indels) discovery workflow (Van der Auwera et al., 2013; DePristo et al., 2011)

4. Results

4. Results

4.1. Quality Checks

FastQC?

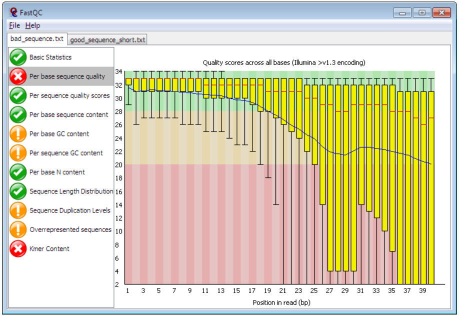

Figure: Example of FastQC Result (Andrews et al., 2012)

- A quality check tool for sequence data
- Give an overview that which test may be problems

FastQC on WES

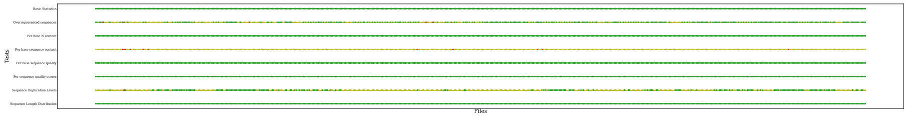

Figure: FastQC with WES data

Failure on 33P1 sample

33P1 is excluded from further analyses.

Failure on 33P1 I

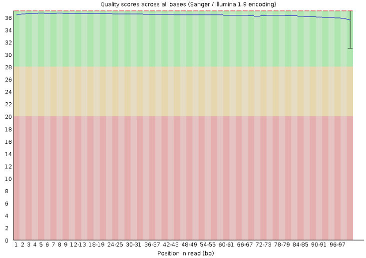

(a) 33N

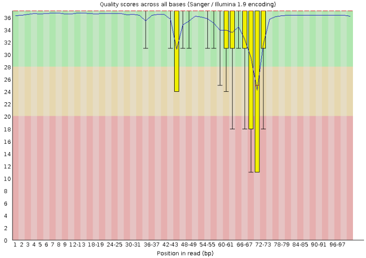

(b) 33P1

Figure: Per Base Sequence Quality Results

Failure on 33P1 II

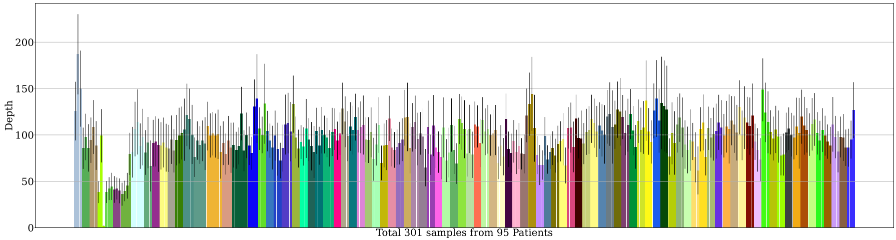

Figure: Coverage Depth Plot

- Tumor DNA: 97.6×; Germline DNA: 95.8× in TCGA LUAD (Duhig et al., 2014)
- Mean 121×, with 83 % of target bases above 30× in TCGA LUSC (Dosenbach et al., 2007)

FastQC on WTS

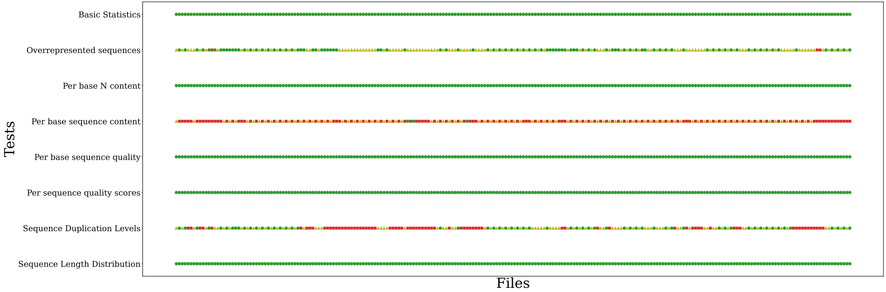

Figure: FastQC with WTS data

All sample are good to analysis

∵ No sample has more than 5 failures.

4. Results

4.2. Quality Checks with Picard

Picard?

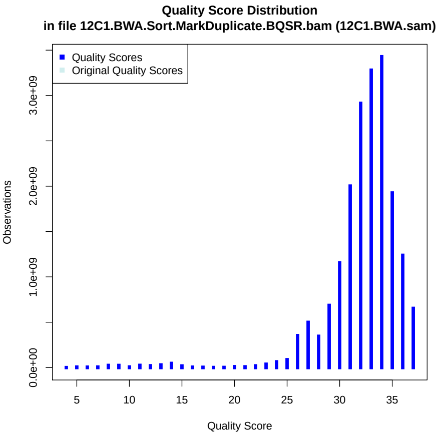

Figure: Quality Distribution of 12C1 sample

Quality Distribution Plot

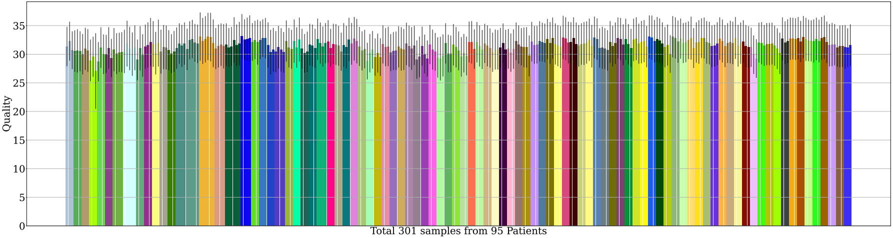

Figure: Quality Distribution by Samples

Findings in Picard

4. Results

4.3. Copy Number Variations

PureCN?

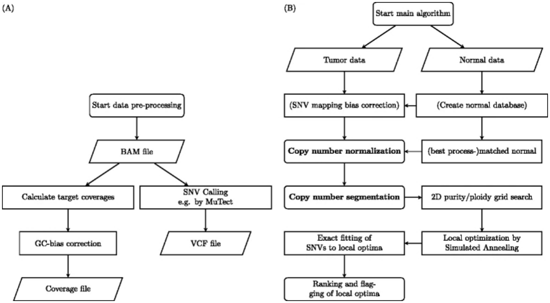

Figure: Flowchart of the PureCN data pre-processing pipeline (Riester et al., 2016)

Purity & Ploidy on WES

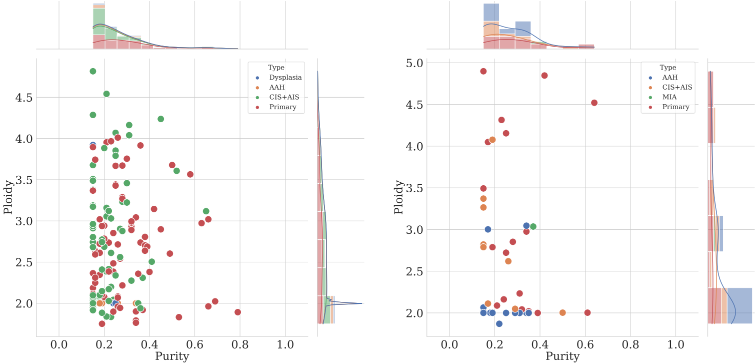

(a) LUSC Samples (b) LUAD Samples

Figure: Cellularity and Ploidy from PureCN

LUSC in CNV Plot I

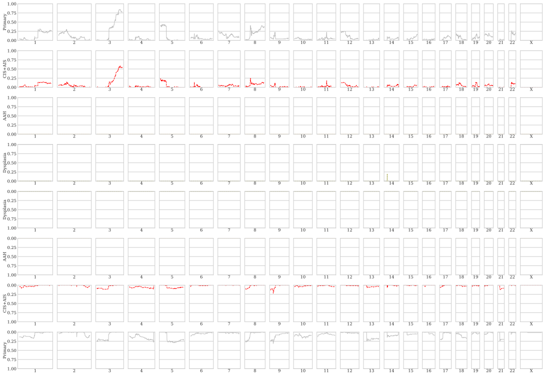

Figure: LUSC in CNV Plot

LUSC in CNV Plot II

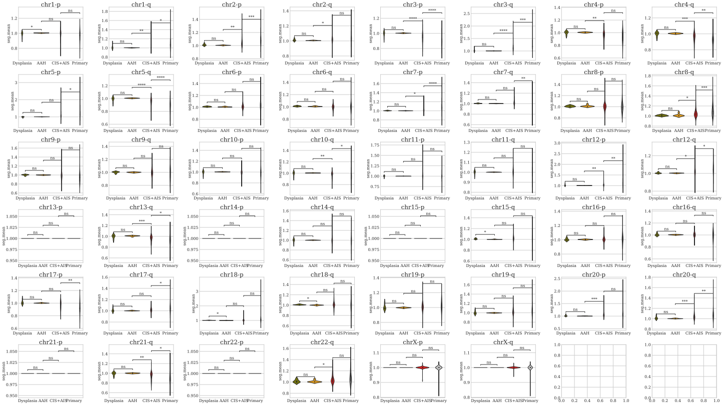

Figure: LUSC in Violin Plots

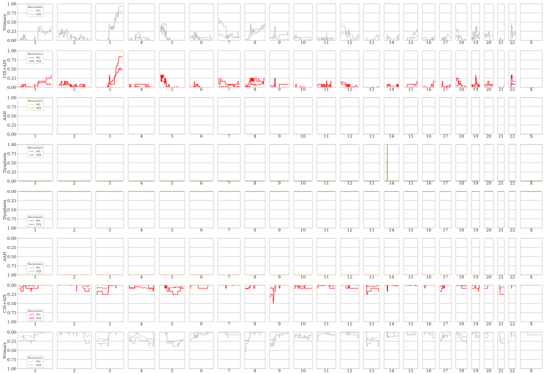

Figure: LUSC with Recurrence in CNV Plot

LUSC with Recurrence in CNV Plot II

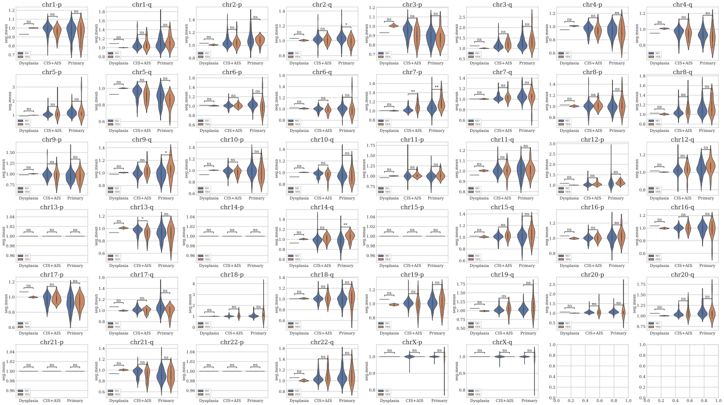

Figure: LUSC with Recurrence in Violin Plots

LUSC with Smoking in CNV Plot I

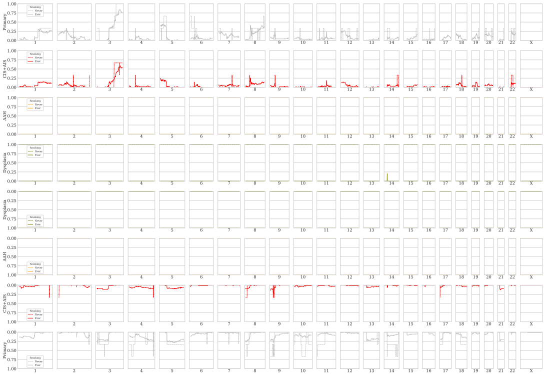

Figure: LUSC with Smoking in CNV Plot

LUSC with Smoking in CNV Plot II

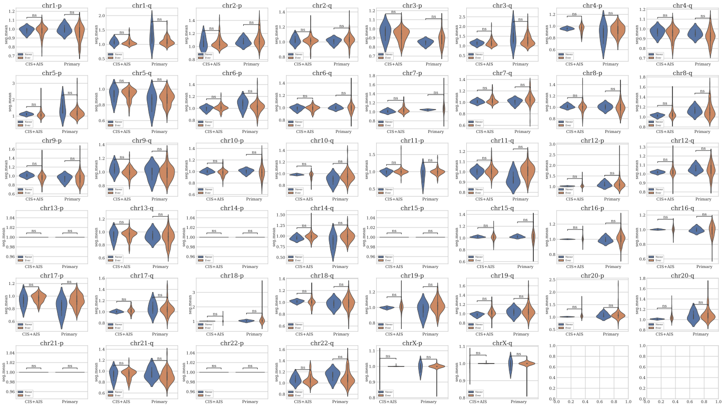

Figure: LUSC with Smoking in Violin Plots

Findings in PureCN with LUSC I

Chr2 p-arm gain

1. Chr2 p-arm gain in Primary.

Table: CGC Tier1 genes in Chr2 p-arm

Gene Symbol (15)	Name
ALK	anaplastic lymphoma kinase (Ki-1)
BCL11A	B-cell CLL/lymphoma 11A
DCTN1	dynactin 1
DNMT3A	DNA (cytosine-5-)-methyltransferase 3 alpha
EML4	echinoderm microtubule associated protein like 4

Findings in PureCN with LUSC II

Chr2 q-arm loss

1. Chr2 q-arm loss in Recurrence & Primary.

Table: CGC Tier1 genes in Chr2 q-arm

Gene Symbol (23)	Name
ACKR3	atypical chemokine receptor 3
ACSL3	acyl-CoA synthetase long-chain family member 3
ACVR1	activin A receptor, type I
ACVR2A	activin A receptor type 2A
AFF3	AF4/FMR2 family, member 3

Findings in PureCN with LUSC III

Chr3 p-arm loss

1. Chr3 p-arm loss in Primary.

Table: CGC Tier1 genes in Chr3 p-arm

Gene Symbol (17)	Name
BAP1	BRCA1 associated protein-1 (ubiquitin carboxy-t...
CACNA1D	calcium channel, voltage-dependent, L type, alp...
CTNNB1	catenin (cadherin-associated protein), beta 1
FANCD2	Fanconi anemia, complementation group D2
FHIT	fragile histidine triad gene

Findings in PureCN with LUSC IV

Chr3 q-arm gain

1. Chr3 q-arm gain in Primary.

Table: CGC Tier1 genes in Chr3 q-arm

Gene Symbol (21)	Name
ATR	ATR serine/threonine kinase
BCL6	B-cell CLL/lymphoma 6
CBLB	Cas-Br-M (murine) ecotropic retroviral transfor...
CNBP	CCHC-type zinc finger, nucleic acid binding pro...
EIF4A2	eukaryotic translation initiation factor 4A, is...

Findings in PureCN with LUSC V

Chr5 q-arm loss

1. Chr5 q-arm loss in Primary.

Table: CGC Tier1 genes in Chr5 q-arm

Gene Symbol (15)	Name
AFF4	AF4/FMR2 family, member 4
APC	adenomatous polyposis of the colon gene
ARHGAP26	Rho GTPase activating protein 26
CD74	CD74 molecule, major histocompatibility complex...
EBF1	early B-cell factor 1

Findings in PureCN with LUSC VI

Chr7 p-arm gain

1. Chr7 p-arm gain in Primary.
2. Chr7 p-arm gain in Recurrence.

Table: CGC Tier1 genes in Chr7 p-arm

Gene Symbol (11)	Name
CARD11	caspase recruitment domain family, member 11
EGFR	epidermal growth factor receptor (erythroblasti...
ETV1	ets variant gene 1
HNRNPA2B1	heterogeneous nuclear ribonucleoprotein A2/B1
HOXA11	homeo box A11

Findings in PureCN with LUSC VII

Chr8 q-arm gain

1. Chr8 q-arm gain in Primary.

Table: CGC Tier1 genes in Chr8 q-arm

Gene Symbol (16)	Name
CHCHD7	coiled-coil-helix-coiled-coil-helix domain cont...
EIF3E	eukaryotic translation initiation factor 3, sub...
EXT1	multiple exostoses type 1 gene
HEY1	hairy/enhancer-of-split related with YRPW motif 1
MYC	v-myc myelocytomatosis viral oncogene homolog (...

Findings in PureCN with LUSC VIII

Chr9 q-arm gain

1. Chr9 q-arm gain in Recurrence & Primary.

Table: CGC Tier1 genes in Chr9 q-arm

Gene Symbol (16)	Name
ABL1	v-abl Abelson murine leukemia viral oncogene ho...
BRD3	bromodomain containing 3
CNTRL	centriolin
FANCC	Fanconi anemia, complementation group C
GNAQ	guanine nucleotide binding protein (G protein),...

Findings in PureCN with LUSC IX

Chr14 q-arm gain

1. Chr14 q-arm gain in Recurrence & Primary.

Table: CGC Tier1 genes in Chr14 q-arm

Gene Symbol (18)	Name
AKT1	v-akt murine thymoma viral oncogene homolog 1
BCL11B	B-cell CLL/lymphoma 11B (CTIP2)
CCNB1IP1	cyclin B1 interacting protein 1, E3 ubiquitin p...
DICER1	dicer 1, ribonuclease type III
FOXA1	forkhead box A1

Findings in PureCN with LUSC X

Chr19 p-arm gain

1. Chr19 p-arm gain in Recurrence & Primary.

Table: CGC Tier1 genes in Chr19 p-arm

Gene Symbol (19)	Name
BRD4	bromodomain containing 4
CALR	calreticulin
CRTC1	CREB regulated transcription coactivator 1
DNAJB1	DnaJ heat shock protein family (Hsp40) member B1
DNM2	dynamin 2

LUAD in CNV Plot I

Figure: LUAD in CNV Plot

LUAD in CNV Plot II

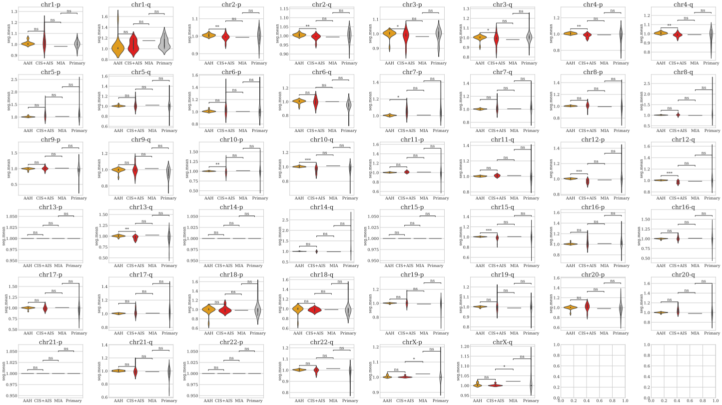

Figure: LUAD in Violin Plots

LUAD with Recurrence in CNV Plot I

Figure: LUAD with Recurrence in CNV Plot

LUAD with Recurrence in CNV Plot II

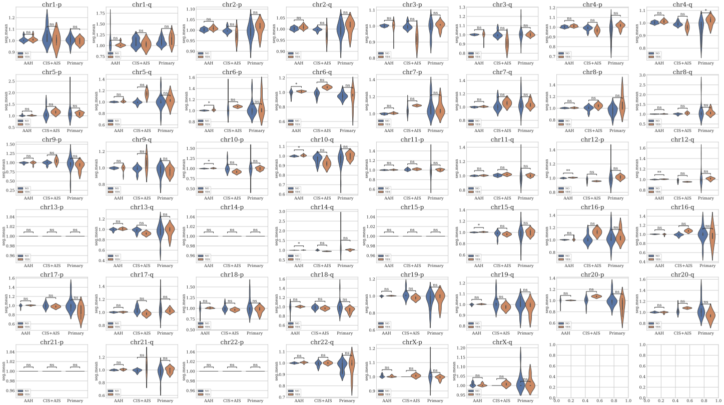

Figure: LUAD with Recurrence in Violin Plots

LUAD with Smoking in CNV Plot I

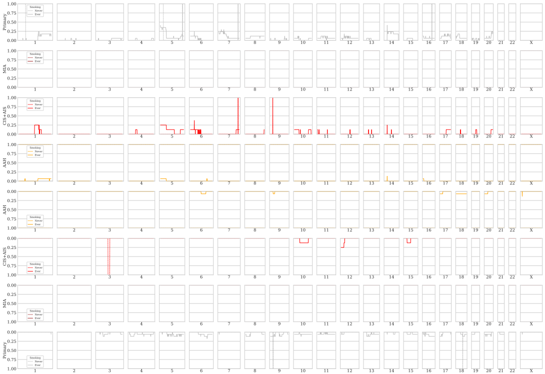

Figure: LUAD with Smoking in CNV Plot

LUAD with Smoking in CNV Plot II

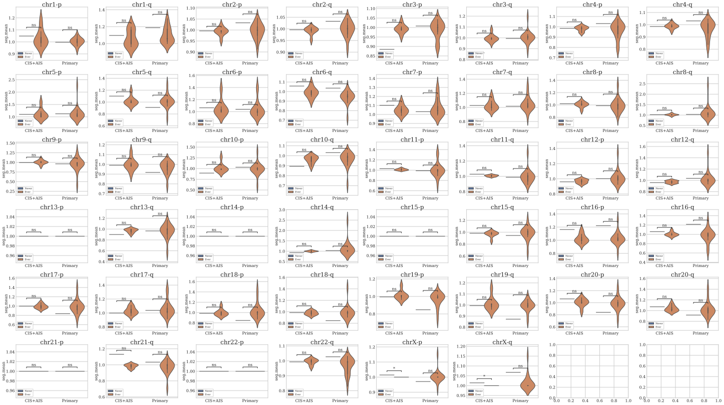

Figure: LUAD with Smoking in Violin Plots

Findings in PureCN with LUAD I

Chr1 q-arm gain

1. Chr1 q-arm gain in Primary.

Table: CGC Tier1 genes in Chr1 q-arm

Gene Symbol (24)	Name
ABL2	c-abl oncogene 2, non-receptor tyrosine kinase
ARNT	aryl hydrocarbon receptor nuclear translocator
BCL9	B-cell CLL/lymphoma 9
CDC73	cell division cycle 73
DDR2	discoidin domain receptor 2

Findings in PureCN with LUAD II

Chr4 q-arm gain

1. Chr4 q-arm gain in Recurrence & Primary.

Table: CGC Tier1 genes in Chr4 q-arm

Gene Symbol (13)	Name
AFF1	AF4/FMR2 family, member 1
FAT1	FAT atypical cadherin 1
FAT4	FAT atypical cadherin 4
FBXW7	F-box and WD-40 domain protein 7 (archipelago h...
FIP1L1	FIP1 like 1 (S. cerevisiae)

Findings in PureCN with LUAD III

Chr5 q-arm gain

1. Chr5 q-arm loss in Non-recurrence & Precancer.

Table: CGC Tier1 genes in Chr5 q-arm

Gene Symbol (15)	Name
AFF4	AF4/FMR2 family, member 4
APC	adenomatous polyposis of the colon gene
ARHGAP26	Rho GTPase activating protein 26
CD74	CD74 molecule, major histocompatibility complex...
EBF1	early B-cell factor 1

Findings in PureCN with LUAD IV

Chr6 p-arm gain

1. Chr6 p-arm gain in Non-recurrence & Precancer.

Table: CGC Tier1 genes in Chr6 p-arm

Gene Symbol (16)	Name
CCND3	cyclin D3
DAXX	death-domain associated protein
DEK	DEK oncogene (DNA binding)
FANCE	Fanconi anemia, complementation group E
HIST1H3B	histone cluster 1, H3b

Findings in PureCN with LUAD V

Chr6 q-arm gain

1. Chr6 q-arm gain in Non-recurrence & Precancer.

Table: CGC Tier1 genes in Chr6 q-arm

Gene Symbol (15)	Name
AFDN	myeloid/lymphoid or mixed-lineage leukemia (tri...
ARID1B	AT rich interactive domain 1B
ESR1	estrogen receptor 1
EZR	ezrin
FGFR1OP	FGFR1 oncogene partner (FOP)

Findings in PureCN with LUAD VI

Chr6 q-arm loss

1. Chr6 q-arm loss in Primary.

Table: CGC Tier1 genes in Chr6 q-arm

Gene Symbol (15)	Name
AFDN	myeloid/lymphoid or mixed-lineage leukemia (tri...
ARID1B	AT rich interactive domain 1B
ESR1	estrogen receptor 1
EZR	ezrin
FGFR1OP	FGFR1 oncogene partner (FOP)

Findings in PureCN with LUAD VII

Chr7 q-arm gain

1. Chr7 q-arm gain in Non-recurrence & Precancer.

Table: CGC Tier1 genes in Chr7 q-arm

Gene Symbol (14)	Name
BRAF	v-raf murine sarcoma viral oncogene homolog B1
CDK6	cyclin-dependent kinase 6
CREB3L2	cAMP responsive element binding protein 3-like 2
CUX1	cut-like homeobox 1
EZH2	enhancer of zeste homolog 2

Findings in PureCN with LUAD VIII

Chr12 p-arm gain

1. Chr12 p-arm loss in Non-recurrence & Primary.

Table: CGC Tier1 genes in Chr12 p-arm

Gene Symbol (10)	Name
CCND2	cyclin D2
CDKN1B	cyclin-dependent kinase inhibitor 1B (p27, Kip1)
CHD4	chromodomain helicase DNA binding protein 4
ERC1	ELKS/RAB6-interacting/CAST family member 1
ETNK1	ethanolamine kinase 1

Findings in PureCN with LUAD IX

Chr12 q-arm gain

1. Chr12 q-arm loss in Non-recurrence & Primary.

Table: CGC Tier1 genes in Chr12 q-arm

Gene Symbol (26)	Name
ARID2	AT rich interactive domain 2
ATF1	activating transcription factor 1
BCL7A	B-cell CLL/lymphoma 7A
BTG1	B-cell translocation gene 1, anti-proliferative
CDK4	cyclin-dependent kinase 4

Findings in PureCN with LUAD X

Chr22 q-arm loss

1. Chr22 q-arm loss in Primary.

Table: CGC Tier1 genes in Chr22 q-arm

Gene Symbol (15)	Name
APOBEC3B	apolipoprotein B mRNA editing enzyme catalytic ...
BCR	breakpoint cluster region
CHEK2	CHK2 checkpoint homolog (S. pombe)
CLTCL1	clathrin, heavy polypeptide-like 1
EP300	300 kd E1A-Binding protein gene

Findings in PureCN

Gistic?

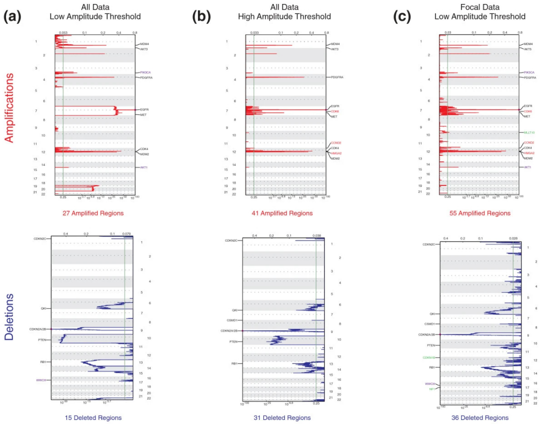

Figure: Effects of arm-level events on GISTIC results (Mermel et al., 2011)

Gistic in LUSC

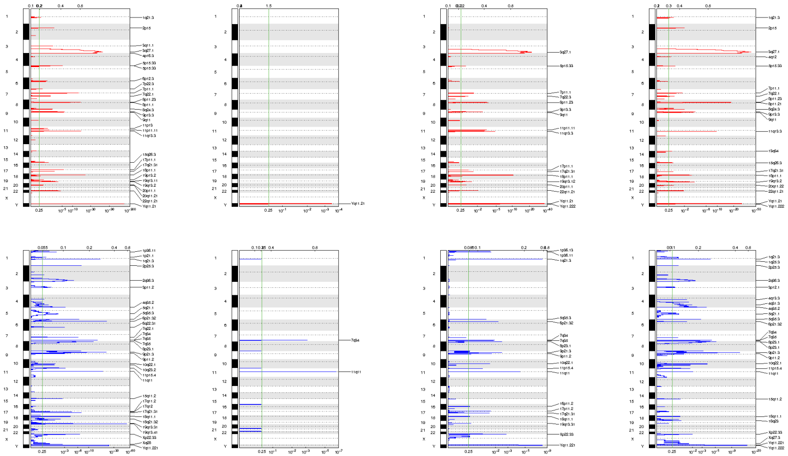

(a) All (b) Dysplasia (c) CIS (d) Primary

Figure: Gistic results in LUSC

Gistic in LUAD

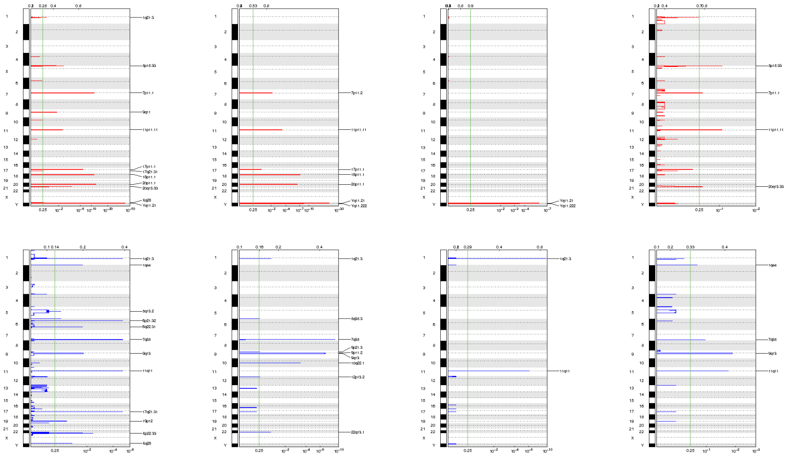

(a) All (b) AAH (c) AIS (d) Primary

Figure: Gistic results in LUAD

Findings in Gistic

4. Results

4.4. Single Nucleotide Variations Analysis

Mutect2?

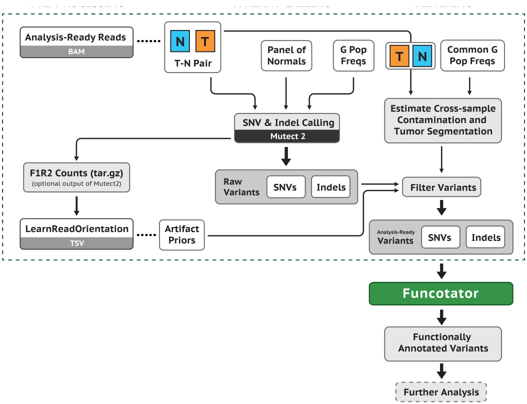

Figure: Somatic short variant discovery workflow (Van der Auwera et al., 2013; DePristo et al., 2011)

MutEnricher?

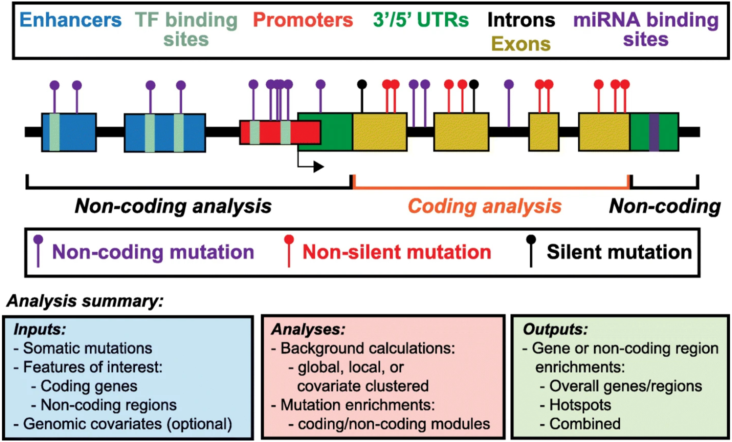

Figure: Schematic representation of MunEnricher's analysis procedures (Soltis et al., 2020)

CoMut?

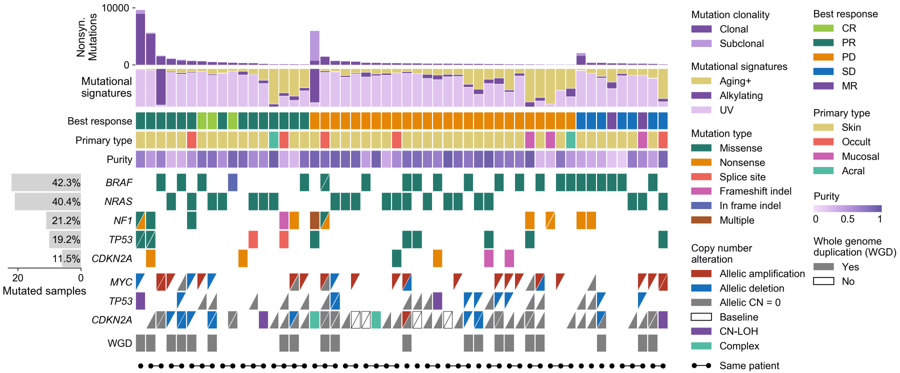

Figure: A comutation plot generated with CoMut (Crowdis et al., 2020)

Driver Gene Selection Strategy

COSMIC Cancer Gene Census (Tate John et al., 2018)

Gene $\in$ CGC Tier 1 set

Fisher FDR

Fisher FDR < 0.05

Fisher P-value

Fisher P-value < 0.05

Gene P-value

Gene P-value < 0.05

Somatic Variant in LUSC

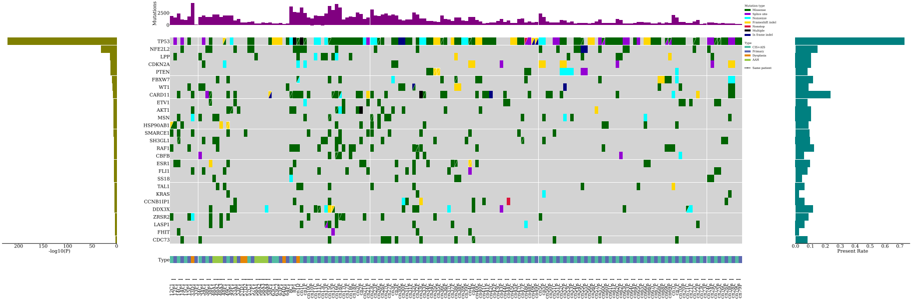

Figure: CoMut Plot with LUSC Patients

Somatic Variant in LUSC with Recurrence

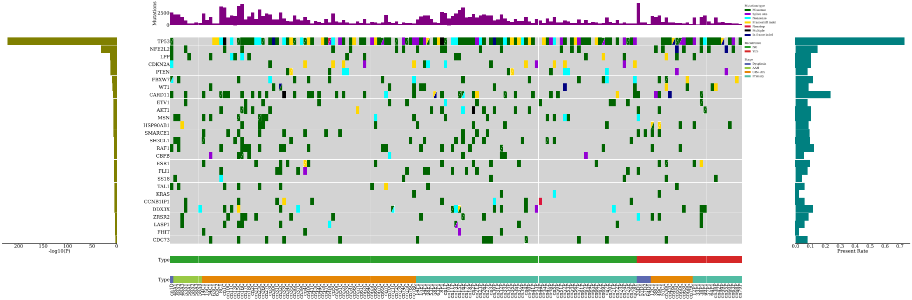

Figure: CoMut Plot in LUSC Patients with Recurrence

Somatic Variant in LUAD

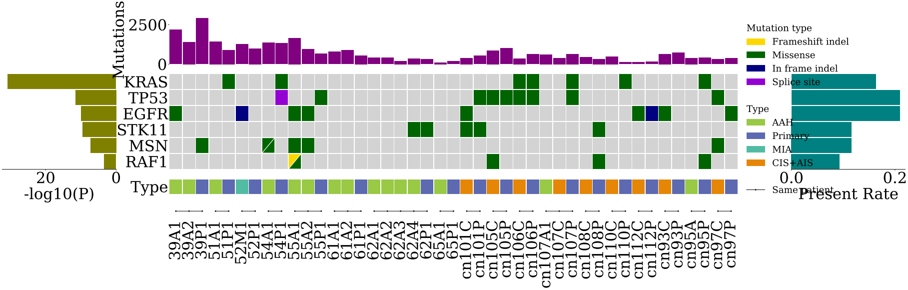

Figure: CoMut Plot with LUAD Patients

Somatic Variant in LUAD with Recurrence

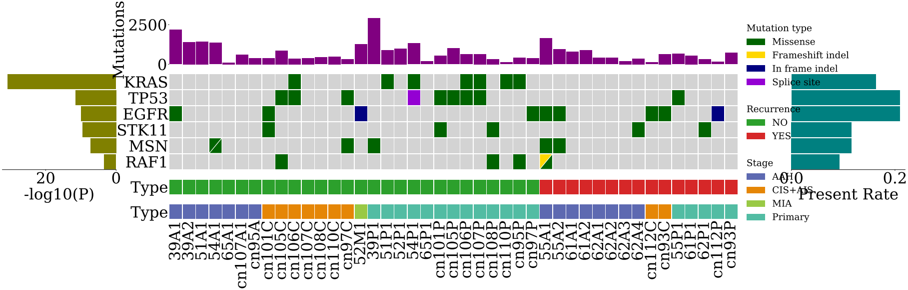

Figure: CoMut Plot in LUAD Patients with Recurrence

Findings in SNVs Analysis

4. Results

4.5. VAF Analysis

VAF?

- Variant allele frequency
- $\text{VAF} = \text{Alternative allele read count}/\text{Total read count}$
- To find tumor evolution

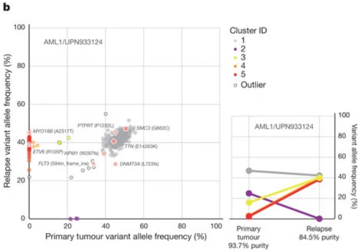

Figure: VAF distribution of validated mutations (Ding et al., 2012)

VAF Plots

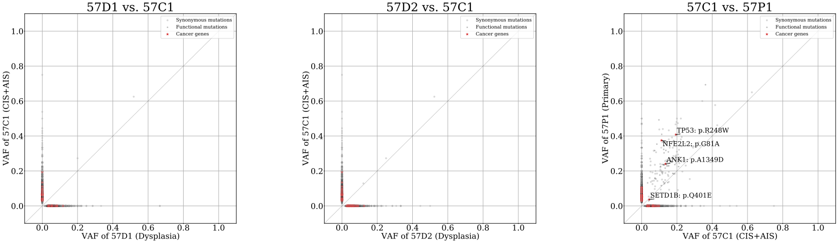

(a) Dysplasia + CIS (b) Dysplasia + CIS (c) CIS + Primary

Figure: VAF plots in patient #57

PyClone?

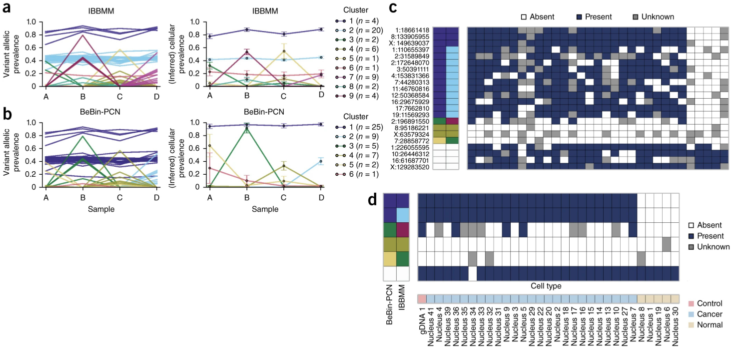

Figure: Analysis of multiple samples by PyClone (Roth et al., 2014)

PyClone Plots I

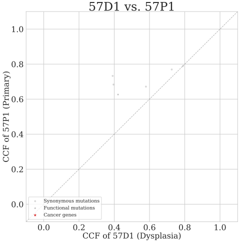

(a) 57D1

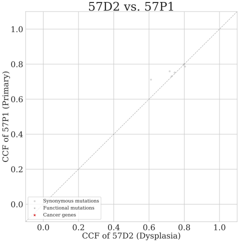

(b) 57D2

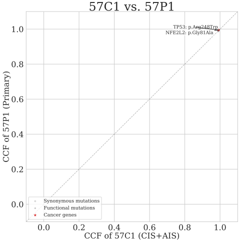

(c) 57C1

Figure: CCF plot in patient #57

PyClone Plots II

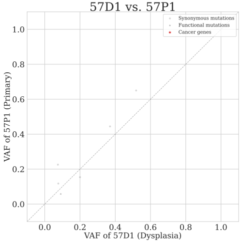

(a) 57D1

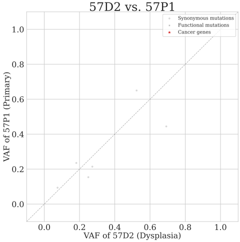

(b) 57D2

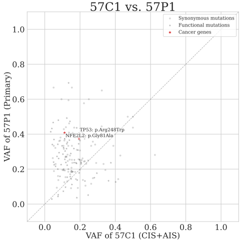

(c) 57C1

Figure: VAF plot in patient #57

Findings in VAF Analysis

4. Results

4.6. Tumor Evolution Trajectories Analysis

Mobster?

Findings in Tumor Evolution Trajectories Analysis

4. Results

4.7. Bulk Cell Deconvolution

BisqueRNA?

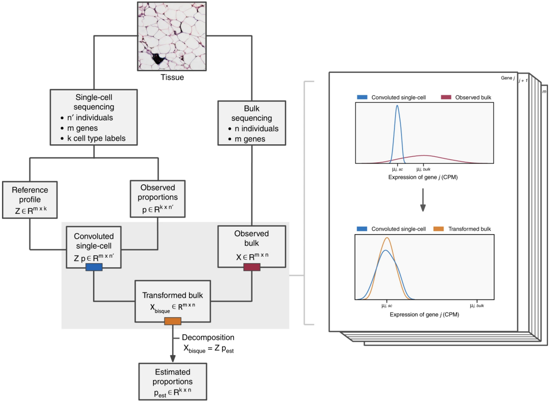

Figure: Workflow for BisqueRNA (Jew et al., 2020)

4. Results

4.7. Bulk Cell Deconvolution

4.7.1. Reference by N. Kim et al. (2020)

Reference Single-cell Data

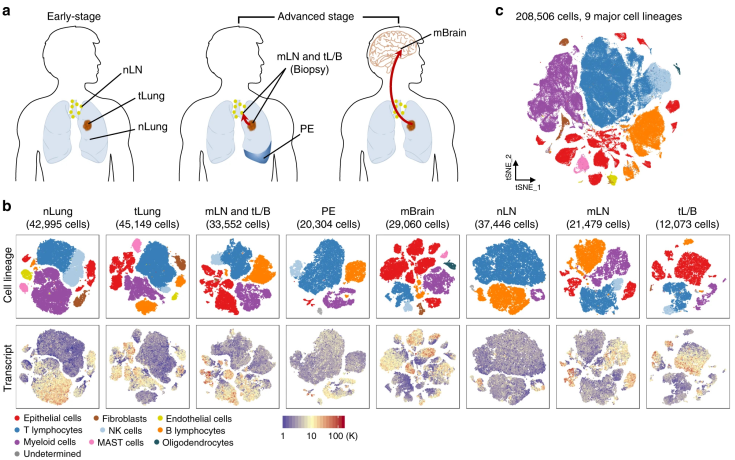

Figure: Comprehensive dissection and clustering of 208,506 single cells from LUAD patients (N. Kim et al., 2020)

Cluster Plot in LUSC

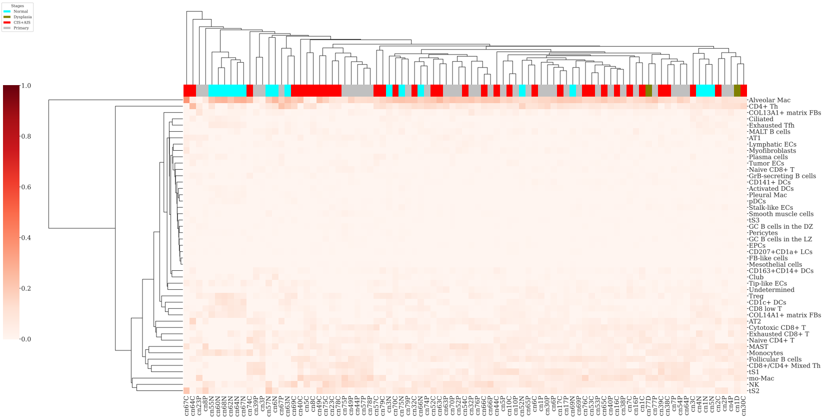

Figure: Cluster Plot in LUSC

Violin Plots in LUSC I

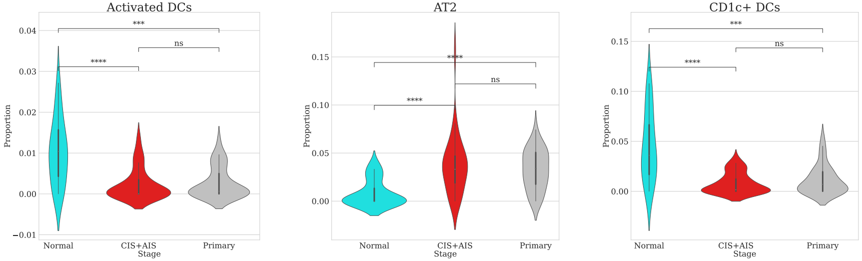

(a) Activated DCs (b) Alveolar type II (c) Langerhans cells

Figure: Violin Plots in LUSC

Violin Plots in LUSC II

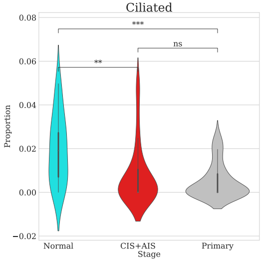

(d) Ciliated cells

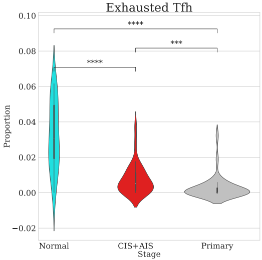

(e) Exhausted T follicular helper

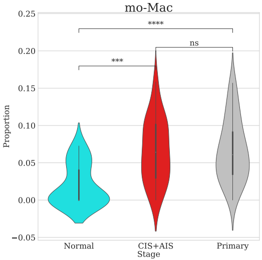

(f) Mo & Mac

Figure: Violin Plots in LUSC

Violin Plots in LUSC III

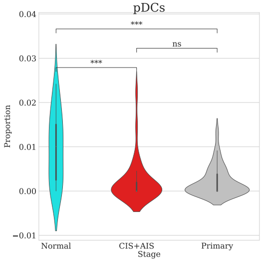

(g) Plasmacytoid DCs

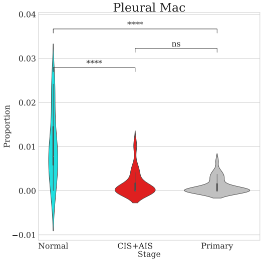

(h) Pleural Mac

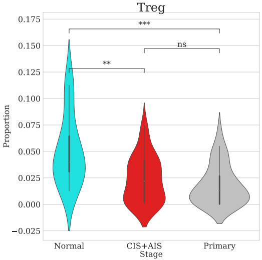

(i) Regulatory T cells

Figure: Violin Plots in LUSC

Violin Plots in LUSC IV

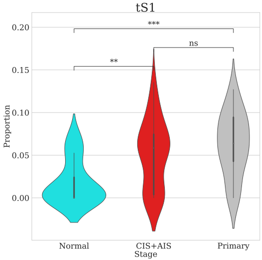

(j) Transcriptional states 1

Figure: Violin Plots in LUSC

Findings in Bulk Cell Deconvolution with LUSC I

Activated DCs

1. Activated DCs have higher proportion in Normal samples.
2. DCs are central regulators of adaptive immune response, *e.g.* anti-tumoral responses .
3. DCs establish a rare immune cell population in tumors .

Alveolar type II

1. Alveolar type II have lower proportion in Normal samples.
2. Alveolar type II proliferate to restore epithelium, and participate in innate immune response (Mason, 2006).
3. Capability of initiating lung cancer development (C. Lin et al., 2012).

Findings in Bulk Cell Deconvolution with LUSC II

CD1c+ DCs (Langerhans cells; LCs)

1. LCs have higher proportion in Normal samples.
2. LCs impact on pathology by inducing tolerance or mediating inflammation (Deckers, Hammad, & Hoste, 2018)
3. LCs facilitate DNA damage and squamous cell carcinoma (Modi et al., 2012)

Ciliated cells

1. Ciliated cells have higher proportion in Normal samples.
2. A terminally differentiated population in lung epithelial cells (Rawlins & Hogan, 2008).
3. Generated under homeostatic condition or response to epithelial injury (Sutherland et al., 2011).

Findings in Bulk Cell Deconvolution with LUSC III

Exhausted T follicular helper cells (Tfh)

1. Exhausted Tfh is gradually decreased along cancer worsen.
2. Tfh cell response is critical for viral infection (Greczmiel et al., 2017; Poonia, Ayithan, Nandi, Masur, & Kottilil, 2018a).
3. Down-regulated Tfh exhaustion correlate with compromise CD8 T-cell immunity (Poonia, Ayithan, Nandi, Masur, & Kottilil, 2018b)

Monocyte & Macrophage

1. Monocyte & Macrophage have lower proportion in Normal samples.
2. Monocyte is a regulator of tumor development & progression (Olingy, Dinh, & Hedrick, 2019).
3. Macrophage is a regulator of link between inflammation & cancer (Sica, Allavena, & Mantovani, 2008).

Findings in Bulk Cell Deconvolution with LUSC IV

Plasmacytoid DCs (pDCs)

1. pDCs have higher proportion in Normal samples.
2. pDCs bring capacities of innate & adaptive immunity (Vermi, Soncini, Melocchi, Sozzani, & Facchetti, 2011).
3. Infiltrated pDCs in neoplasms $\Rightarrow$ Poor prognosis (Pinto, Rega, Crother, & Sorrentino, 2012).

Pleural Macrophages

1. Pleural macrophages have higher proportion in Normal samples.
2. Neutrophil recruitment in pleural inflammation (Cailhier et al., 2006).

Findings in Bulk Cell Deconvolution with LUSC V

Regulatory T cells (Tregs)

1. Tregs have higher proportion in Normal samples.
2. Elevation of Tregs $\Uparrow$ in solid tumors & hematologic malignancies (Beyer & Schultze, 2006).
3. Increasing Tregs $\Uparrow$ along metastatic stage in NSCLC (Erfani et al., 2012) ??.

Tumor cell states 1 (tS1)

1. tS1 have lower proportion in Normal samples.
2. Represent a de-regulation of normal differentiation programs (N. Kim et al., 2020).

Cluster Plot in LUAD

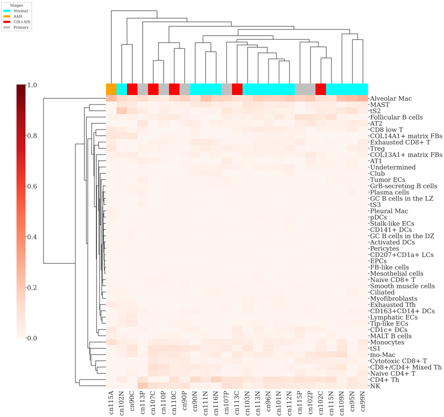

Figure: Cluster Plot in LUAD

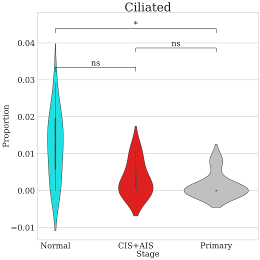

(a) Ciliated cells

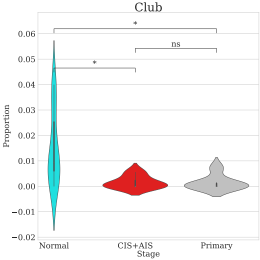

(b) Club Cell

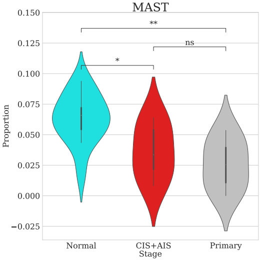

(c) Mast cell

Figure: Violin Plots in LUAD

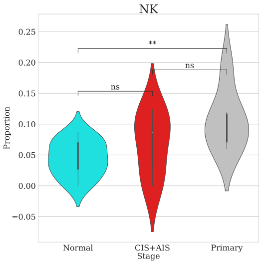

(d) NK cells

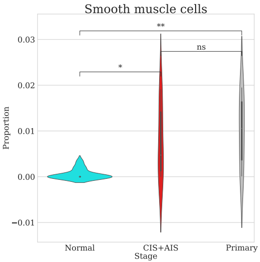

(e) Smooth muscle cells

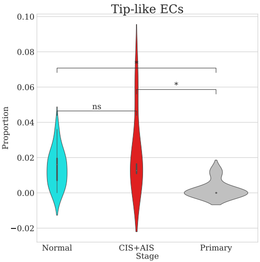

(f) Tip-like ECs

Figure: Violin Plots in LUAD

Findings in Bulk Cell Deconvolution with LUAD I

Cilited cells

1. Cilited cells have higher proportion in Normal than Primary samples.
2. A terminally differentiated population in lung epithelial cells (Rawlins & Hogan, 2008).
3. Generated under homeostatic condition or response to epithelial injury (Sutherland et al., 2011).

Findings in Bulk Cell Deconvolution with LUAD II

Club cells

1. Club cells have higher proportion in Normal than Primary samples.
2. Club cells form LUAD in adult mice (Spella et al., 2019).
3. Club cells in smoking-associated LUAD (Behrend, Giotopoulou, Spella, & Stathopoulos, 2021).
4. Increasing club cells $\Rightarrow$ Good indicator of advanced bronchopulmonary dysplasia (Rokicki, Rokicki, Wojtacha, & Dżeljijli, 2016).

Mast cells

1. Mast cells have higher proportion in Normal than Primary samples.
2. Mast cells activated by lung cancer-derived extracellular vesicles (Xiao et al., 2019).
3. Mast cell promote $\Uparrow$ tumor metastasis (Salamon, Mekori, & Shefler, 2020).

Natural Killer cells (NK cells)

1. NK cells have higher proportion in Primary than Normal samples.
2. NK cells play a major role in innate immune system (Shin et al., 2020a).
3. NK cells can induce immune response against tumor cells (Shin et al., 2020b).
4. NK cells may induce tumor regression in lung cancer (Aktaș et al., 2018) ??.

Findings in Bulk Cell Deconvolution with LUAD IV

Smooth muscle cells

1. Smooth muscle cells have higher proportion in Primary than Normal samples.
2. Hypoxia is a characteristic feature of solid tumors (Brahimi-Horn, Chiche, & Pouysségur, 2007; Vaupel & Mayer, 2007).
3. $\therefore$ Smooth muscle cells pathway is up-regulated in cancer (Kyotani, Takasawa, & Yoshizumi, 2019; T.-T. Zhu et al., 2019).

Tip-like endothelial cells (ECs)

1. Tip-like ECs have lower proportion in Primary than Normal samples.
2. Tip-like ECs were determined into migratory & basement-membrane remodeling phenotypes (Goveia et al., 2020).
3. Tip-like ECs replaced with immature ones in NSCLC (E. Y. Kim et al., 2022).

4. Results

4.7. Bulk Cell Deconvolution

4.7.2. Reference by Gueguen et al. (2021)

Reference Single-cell Data

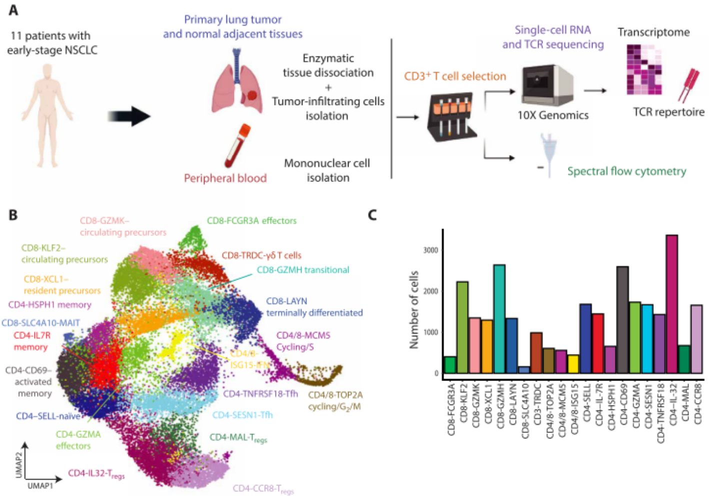

Figure: Characterization of CD3$^+$ TILs in NSCLC (Gueguen et al., 2021)

Cluster Plots in LUSC

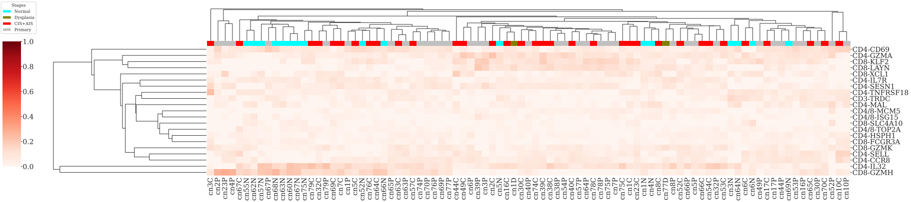

Figure: Cluster Plot in LUAD

Violin Plots in LUSC I

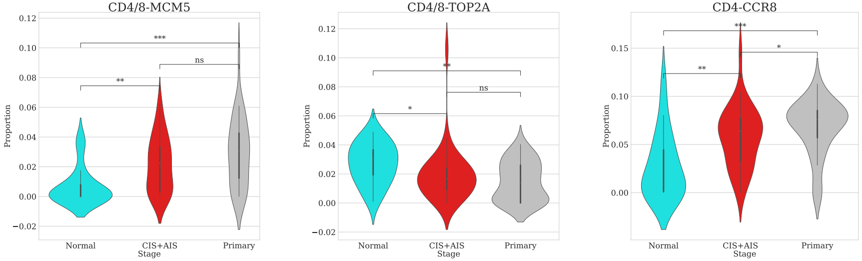

(a) CD4/8-MCM5 (b) CD4/8-TOP2A (c) CD4-CCR8

Figure: Violin Plots in LUSC

Violin Plots in LUSC II

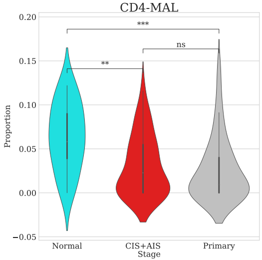

(d) CD4-MAL

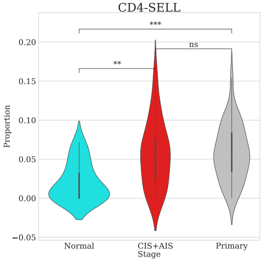

(e) CD4-SELL

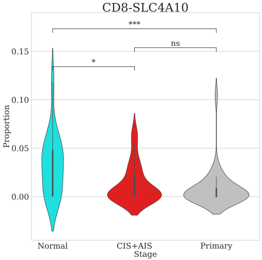

(f) CD8-SLC4A10

Figure: Violin Plots in LUSC

Findings in Bulk Cell Deconvolution with LUSC I

CD4/8-MCM5

1. CD4/8-MCM5 have lower proportion in Normal.
2. MCM5, mini-chromosome maintenance protein 5, acts as component of MCM complex (Tsuji, Ficarro, & Jiang, 2006).
3. MCM5, thus, play a major role in replication and cell cycle progression (Paul, Hu, Musahl, Hameister, & Knippers, 1996).
4. MCM5 could be adverse prognostic marker for NSCLC (Grzegrzolka et al., 2021) and lung cancer (Y.-Z. Liu et al., 2017).

Findings in Bulk Cell Deconvolution with LUSC II

CD4/8-TOP2A

1. CD4/8-TOP2A have higher proportion in Normal.
2. TOP2A, topoisomerase IIA, have an essential role for modulating DNA topology & cell division (Wyles, Wu, Mirski, & Cole, 2007).
3. TOP2A over-expressed $\Uparrow$ in bladder cancer (Zeng et al., 2019), LUAD (Kou et al., 2020) and NSCLC (W. Ma et al., 2019) ??

CD4-CCR8

1. CD4-CCR8 is gradually increased along tumor progression.
2. CCR8, C-C chemokine receptor type 8, might modulate monocyte chemotaxis and tymic cell line apoptosis (Tiffany et al., 1997).
3. CCR8 up-regulated along tumor progression in bladder (X. Liu et al., 2019), colon (Villarreal et al., 2018), and breast cancer (Plitas et al., 2016).

Findings in Bulk Cell Deconvolution with LUSC III

CD4-MAL

1. CD4-MAL have lower proportion in Primary.
2. MAL, myelin and lymphocyte protein, play a role in indirect route for egress of transcytosing cargo (de Marco et al., 2002).
3. Over-expression of MAL was correlated with worse prognostic factors in uterine carcinoma (D. Li et al., 2021).
4. MAL was highly methylated in gastric cancer (Choi et al., 2017).
5. MAL acts as a tumor suppressor or a tumor progression factor among cancer types (Lara-Lemus, 2019).

Findings in Bulk Cell Deconvolution with LUSC IV

CD4-SELL

1. CD4-SELL have higher proportion in Primary.
2. SELL, a calcium-dependent lectin, controls cell adhesion with neighboring cells (Bernimoulin et al., 2003; Wedepohl et al., 2017).
3. SELL over-expressed in breast cancer (Kumari et al., 2021).

CD8-SLC4A10

1. CD8-SLC4A10 have lower proportion in Primary.
2. SLC4A10, sodium-driven chloride bicarbonate exchanger, have an essential role in regulating intracellular pH (C.-Z. Wang, Yano, Nagashima, & Seino, 2000).

Cluster Plots in LUAD

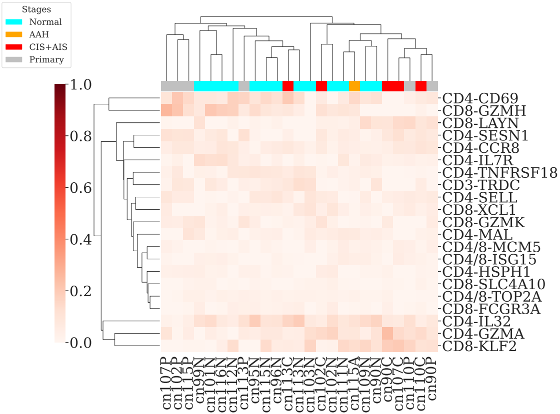

Figure: Cluster Plot in LUAD

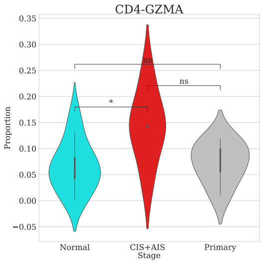

(a) CD4-GZMA

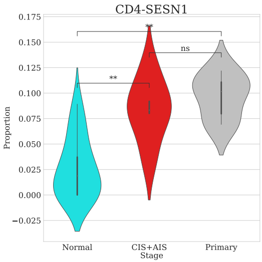

(b) CD4-SESN1

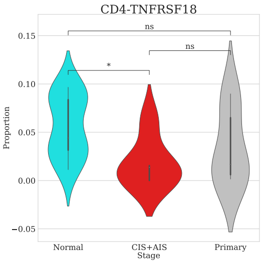

(c) CD4-TNFRSF18

Figure: Violin Plots in LUAD

Findings in Bulk Cell Deconvolution with LUAD I

CD4-GZM

1. CD4-GZM have higher proportion in AIS than Normal.

CD4-SESN1

1. CD4-SESN1 have higher proportion in AIS than Normal.

CD4-TNFRSF18

1. CD4-TNFRSF18 have lower proportion in AIS than Normal.

Findings in Bulk Cell Deconvolution

4. Results

4.8. Discovery of Mutational Signature

Mutational Signature?

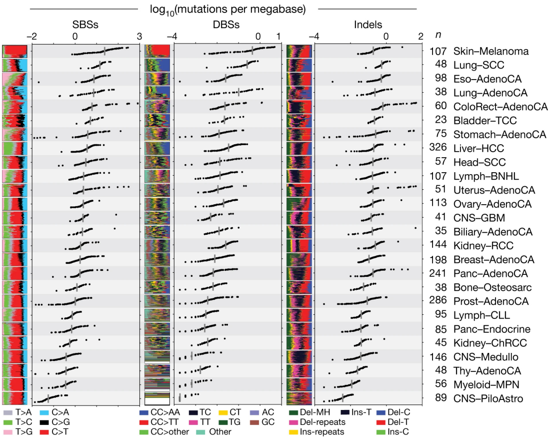

Figure: Mutation Burdens across PCAWG tumor types (Alexandrov et al., 2020)

SigProfiler?

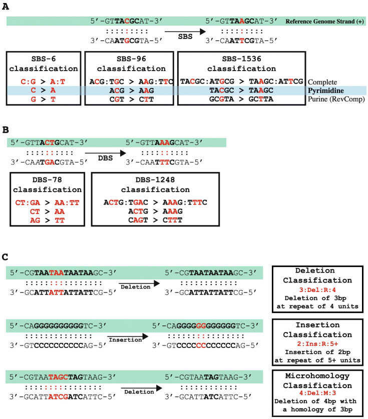

Figure: Classification of mutation signatures by SigProfiler (Bergstrom et al., 2019; Islam et al., 2021; Bergstrom et al., 2020)

4. Results

4.8. Discovery of Mutational Signature

4.8.1. Single Base Substitutions (SBS)

SBS Signatures I

SBS1

- An endogenous mutational process (Nik-Zainal et al., 2012a)
- generates G>T mismatches in double-stranded DNA
- Failure ⇓ to detect & remove these mismatches

SBS2

- Activity of the AID/APOBEC family of cytidine deaminases (Nik-Zainal et al., 2012a)
  1. APOBEC3A is probably responsible in human cancer
  2. APOBEC3B may also contribute
- may be generated directly by DNA replication

SBS Signatures II

SBS4

- Tobacco smoking (Alexandrov et al., 2013)
- Exposed to tabacco carcinogens *e.g.* benzopyrene

SBS5

- Unknown (Alexandrov et al., 2013)
- SBS5 $\Uparrow$ in bladder cancer
- SBS5 $\Uparrow$ in many cancer types $\because$ Tobacco smoking

SBS10b

- Polymerase ϵ exonuclease domain mutations (Alexandrov et al., 2020)

SBS Signatures III

SBS13

- Activity of the AID/APOBEC family of cytidine deaminases (Nik-Zainal et al., 2012b)
- SBS13 is usually found with SBS2

SBS87

- Thiopurine chemotherapy treatment (B. Li et al., 2020)

SBS in LUSC I

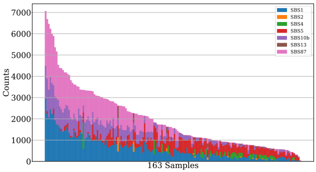

(a) Absolute

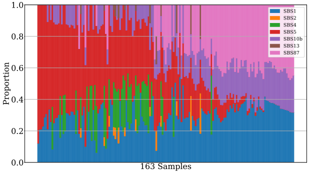

(b) Relative

Figure: SBS Bar Plot in LUSC

SBS in LUSC II

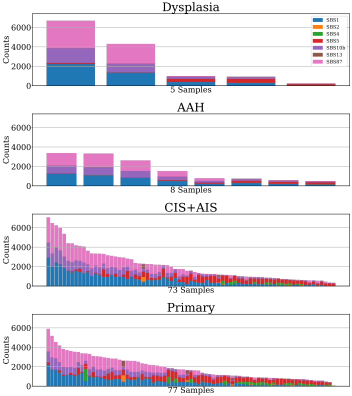

(a) Absolute

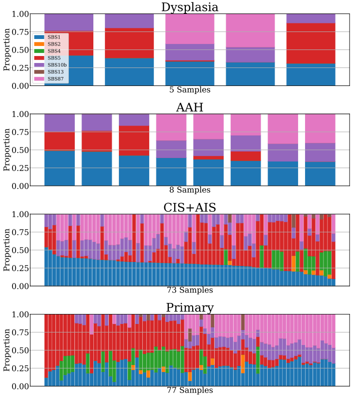

(b) Relative

Figure: SBS Bar Plot by Cancer Subtype in LUSC

SBS in LUSC with Smoking I

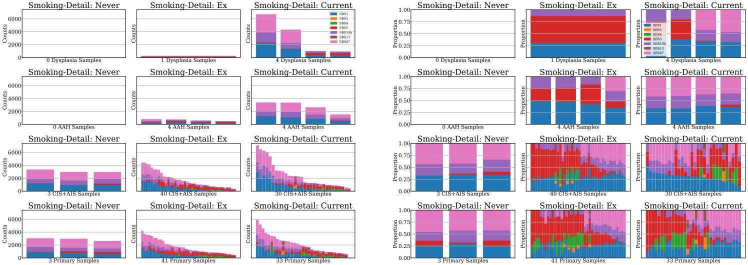

(a) Absolute (b) Relative

Figure: SBS Bar Plot by Cancer Subtype & Smoking in LUSC

SBS in LUSC with Smoking II

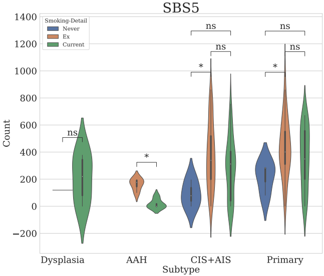

(a) Absolute

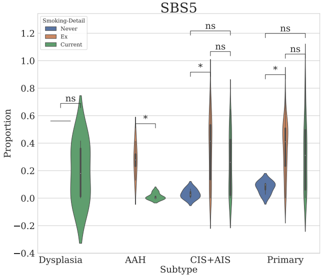

(b) Relative

Figure: SBS5 Signature in LUSC with Smoking

SBS in LUSC with Smoking III

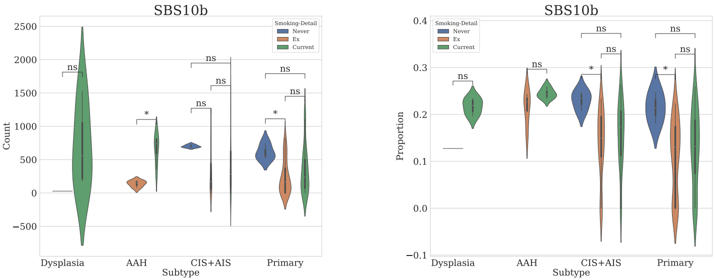

(a) Absolute

(b) Relative

Figure: SBS10b Signature in LUSC with Smoking

SBS in LUSC with Smoking IV

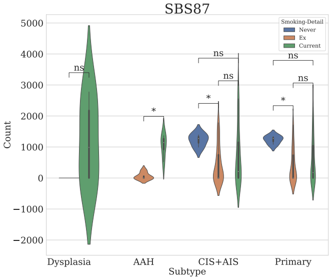

(a) Absolute

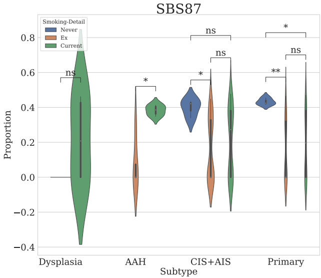

(b) Relative

Figure: SBS87 Signature in LUSC with Smoking

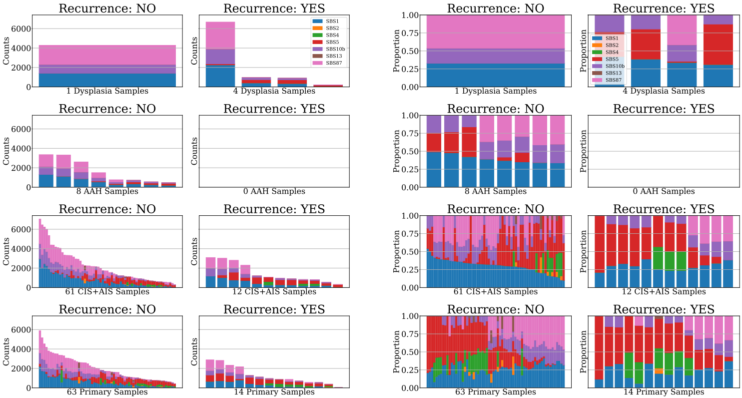

(a) Absolute (b) Relative

Figure: SBS Bar Plot by Cancer Subtype & Recurrence in LUSC

SBS in LUSC with Recurrence II

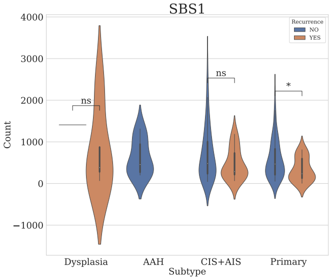

(a) Absolute

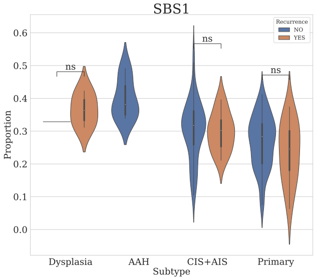

(b) Relative

Figure: SBS1 Signature in LUSC with Recurrence

SBS in LUAD I

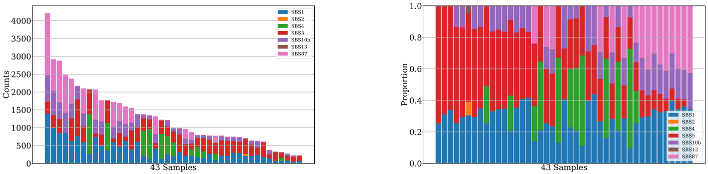

(a) Absolute

(b) Relative

Figure: SBS Bar Plot in LUSC

SBS in LUAD II

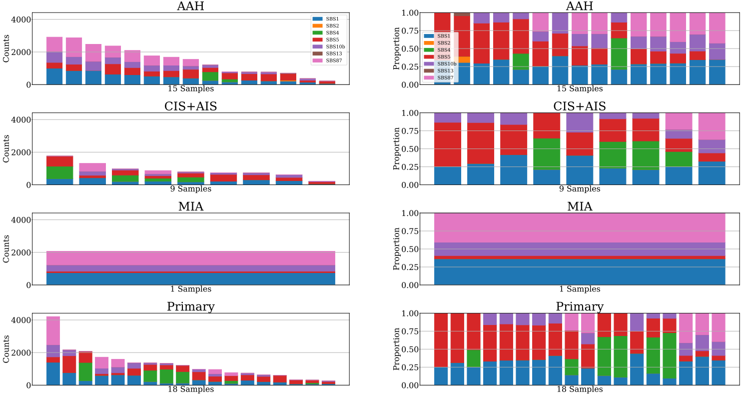

(a) Absolute (b) Relative

Figure: SBS Bar Plot by Cancer Subtype in LUSC

SBS in LUAD with Smoking I

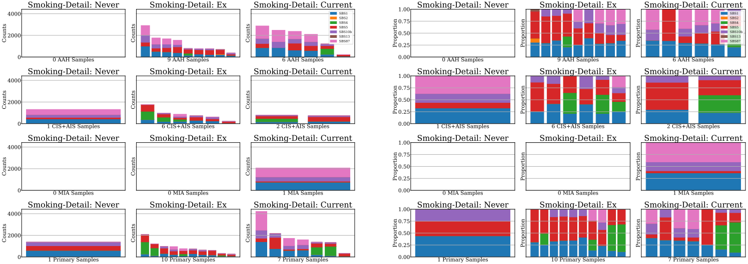

(a) Absolute (b) Relative

Figure: SBS Bar Plot by Cancer Subtype & Smoking in LUAD

SBS in LUAD with Smoking II

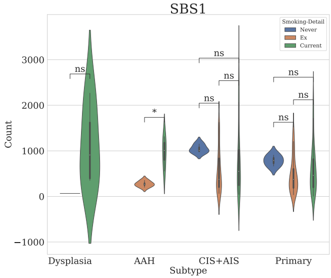

(a) Absolute

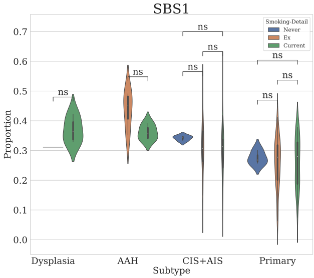

(b) Relative

Figure: SBS1 Signature in LUAD with Smoking

SBS in LUAD with Smoking III

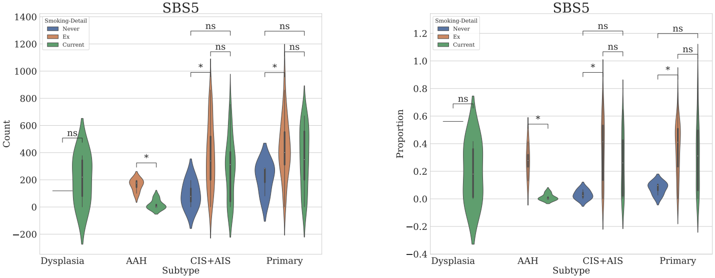

(a) Absolute (b) Relative

Figure: SBS5 Signature in LUAD with Smoking

SBS in LUAD with Smoking IV

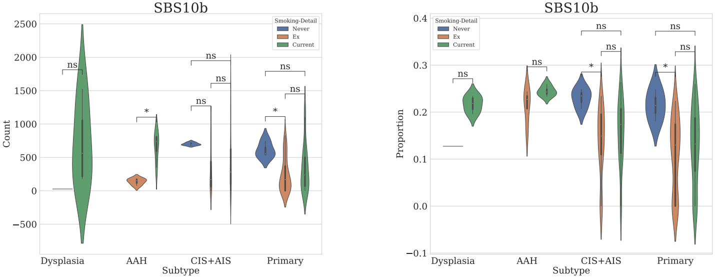

(a) Absolute (b) Relative

Figure: SBS10b Signature in LUAD with Smoking

SBS in LUAD with Smoking V

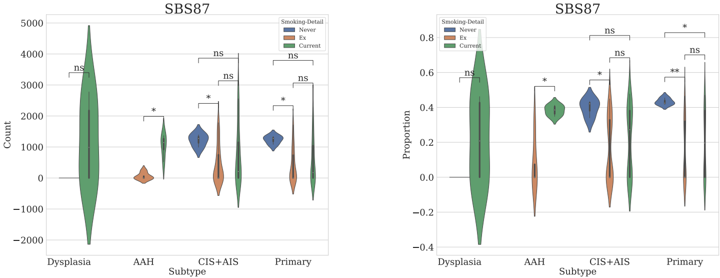

(a) Absolute (b) Relative

Figure: SBS87 Signature in LUAD with Smoking

SBS in LUAD with Recurrence I

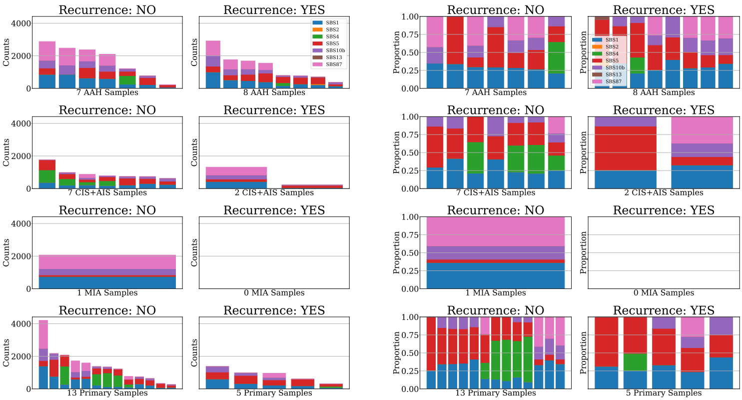

(a) Absolute (b) Relative

Figure: SBS Bar Plot by Cancer Subtype & Recurrence in LUAD

SBS in LUAD with Recurrence II

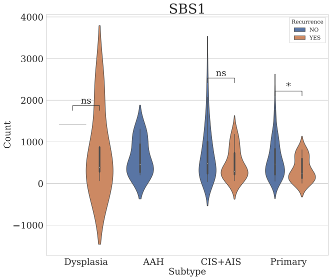

(a) Absolute

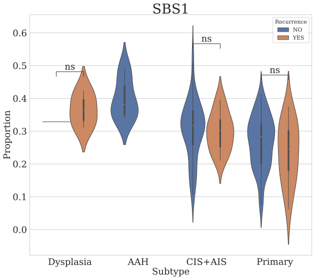

(b) Relative

Figure: SBS1 Signature in LUAD with Recurrence

4. Results

4.8. Discovery of Mutational Signature

4.8.2. Double Base Substitutions (DBS)

DBS Signatures I

DBS2

- Tobacco smoking (J.-M. Chen, Férec, & Cooper, 2013)
- Other endogenous/exogenous mutagens *e.g.* acetaldehyde

DBS7

- Defective $\Downarrow$ DNA mismatch repair (Alexandrov et al., 2020)

DBS78A

content...

DBS in LUSC I

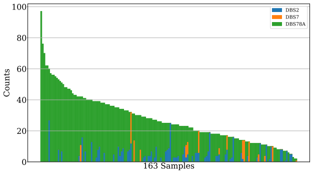

(a) Absolute

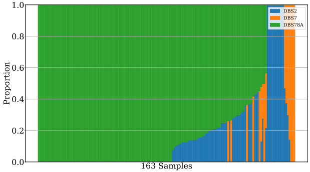

(b) Relative

Figure: DBS Bar Plot in LUSC

DBS in LUSC II

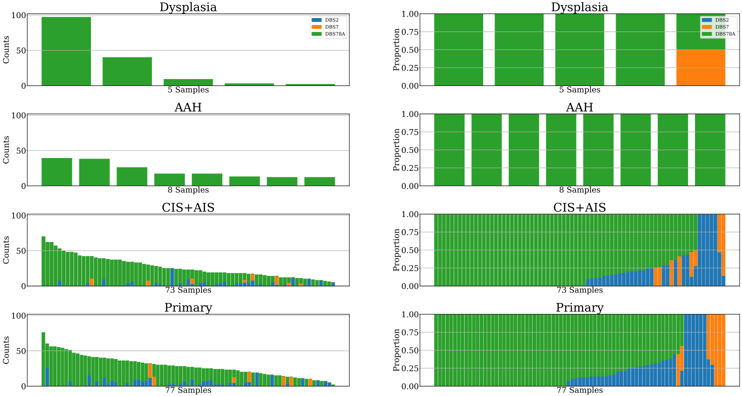

(a) Absolute (b) Relative

Figure: DBS Bar Plot by Cancer Subtype in LUSC

DBS in LUSC III

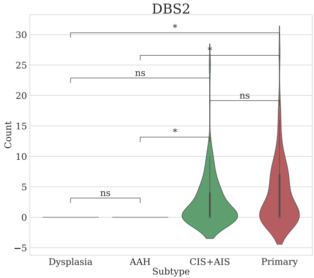

(a) Absolute

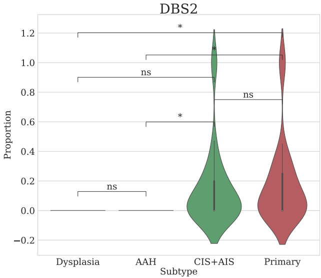

(b) Relative

Figure: DBS2 Signature in LUSC

DBS in LUSC IV

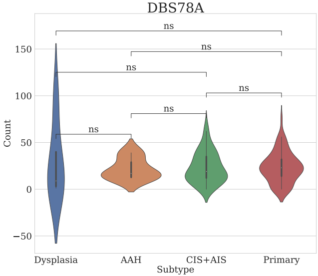

(a) Absolute

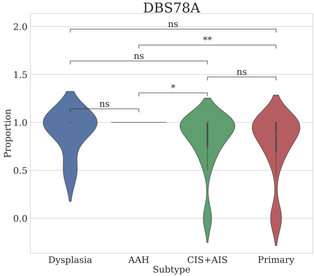

(b) Relative

Figure: DBS78A Signature in LUSC

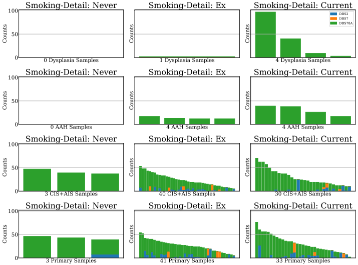

(a) Absolute

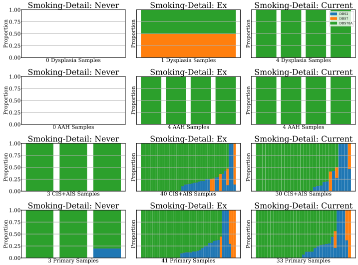

(b) Relative

Figure: DBS Bar Plot by Cancer Subtype & Smoking in LUSC

DBS in LUSC with Smoking II

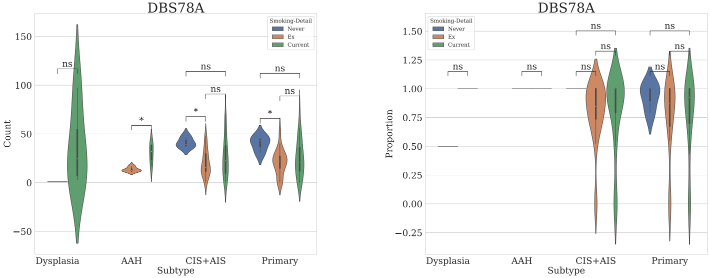

(a) Absolute (b) Relative

Figure: DBS78A Signature in LUSC with Smoking

DBS in LUSC with Recurrence

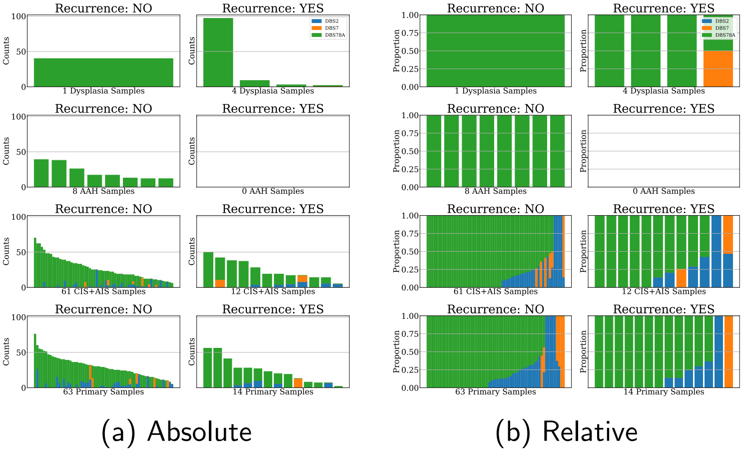

Figure: DBS Bar Plot by Cancer Subtype & Recurrence in LUSC

DBS in LUAD I

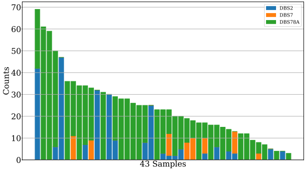

(a) Absolute

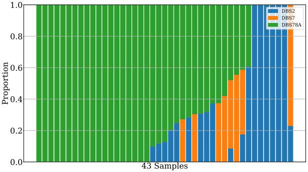

(b) Relative

Figure: DBS Bar Plot in LUAD

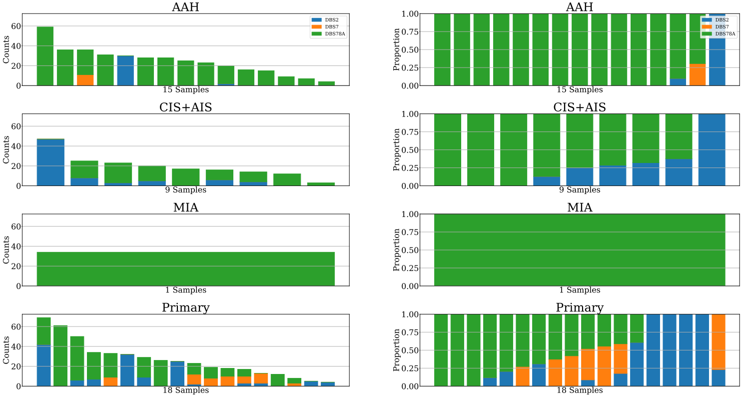

(a) Absolute (b) Relative

Figure: DBS Bar Plot by Cancer Subtype in LUAD

DBS in LUAD III

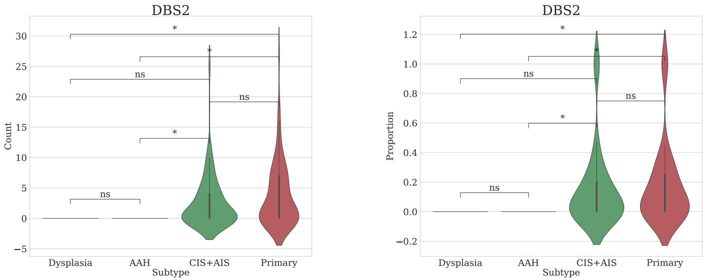

(a) Absolute (b) Relative

Figure: DBS2 Signature in LUSC

DBS in LUAD IV

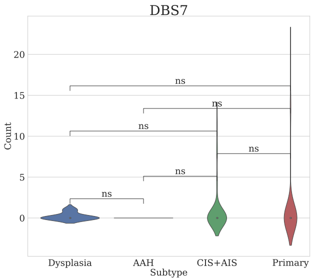

(a) Absolute

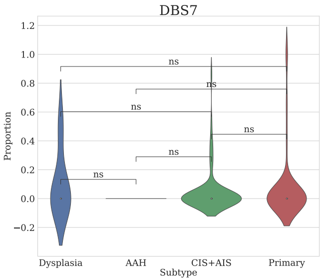

(b) Relative

Figure: DBS7 Signature in LUSC

DBS in LUAD V

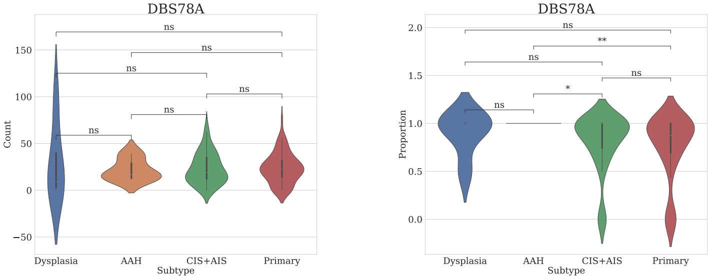

(a) Absolute (b) Relative

Figure: DBS78A Signature in LUSC

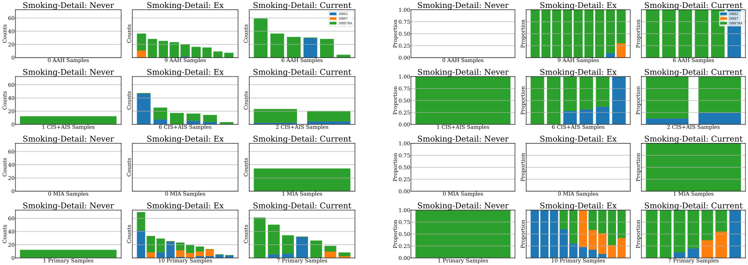

(a) Absolute (b) Relative

Figure: DBS Bar Plot by Cancer Subtype & Smoking in LUAD

DBS in LUAD with Smoking II

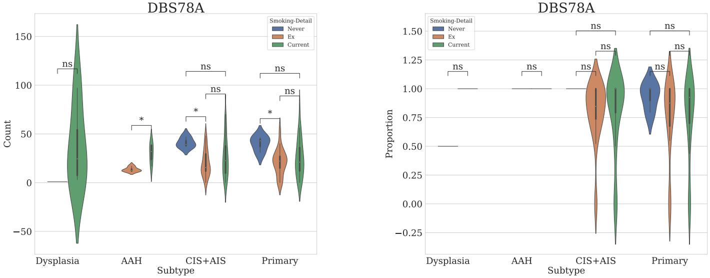

(a) Absolute (b) Relative

Figure: DBS78A Signature in LUSC in Smoking

DBS in LUAD with Recurrence

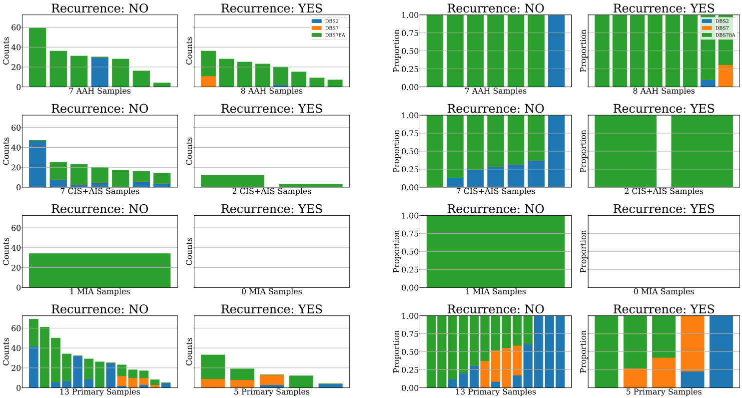

(a) Absolute

(b) Relative

Figure: DBS Bar Plot by Cancer Subtype & Recurrence in LUAD

4. Results

4.8. Discovery of Mutational Signature

4.8.3. Short insertions & Deletions (Indels)

Indel signatures I

ID83A

content...

ID83B

content...

Indels in LUSC I

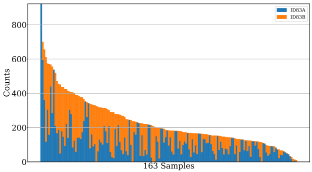

(a) Absolute

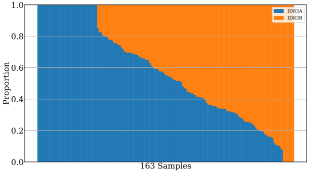

(b) Relative

Figure: Indel Bar Plot in LUSC

Indels in LUSC II

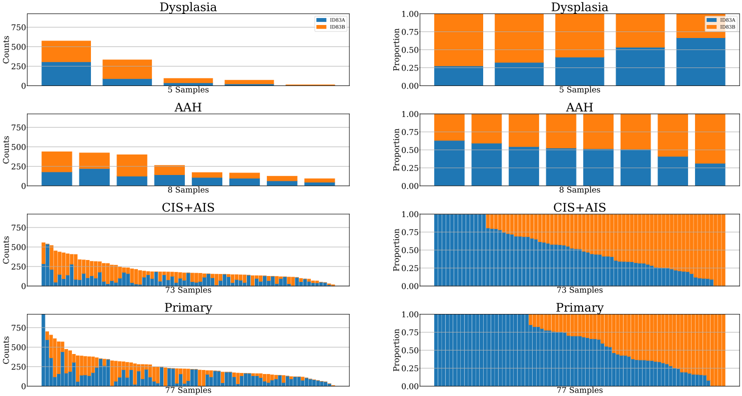

(a) Absolute (b) Relative

Figure: Indel Bar Plot by Cancer Subtype in LUSC

Indels in LUSC III

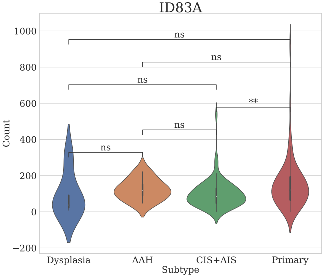

(a) Absolute

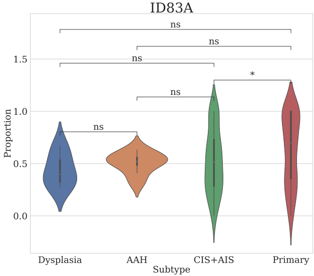

(b) Relative

Figure: Indel83A Signature in LUSC

Indels in LUSC IV

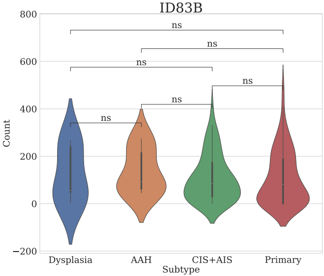

(a) Absolute

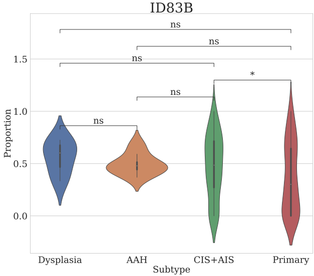

(b) Relative

Figure: Indel83B Signature in LUSC

Indel in LUSC with Smoking I

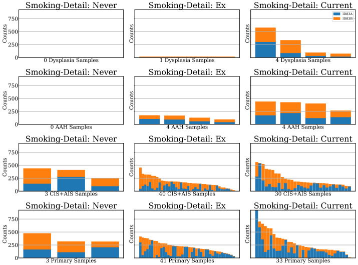

(a) Absolute

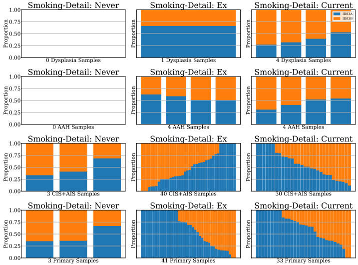

(b) Relative

Figure: Indel Bar Plot by Cancer Subtype & Smoking in LUSC

Indel in LUSC with Smoking II

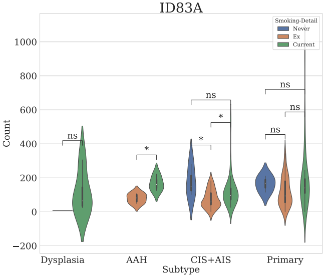

(a) Absolute

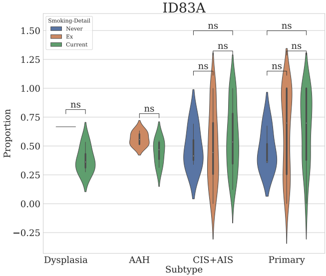

(b) Relative

Figure: Indel83A Signature in LUSC with Smoking

Indel in LUSC with Recurrence

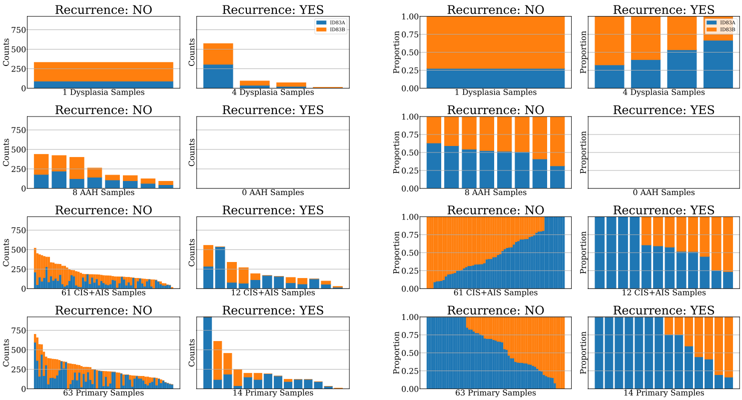

(a) Absolute (b) Relative

Figure: Indel Bar Plot by Cancer Subtype & Recurrence in LUSC

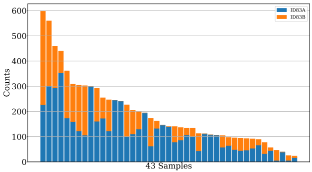

(a) Absolute

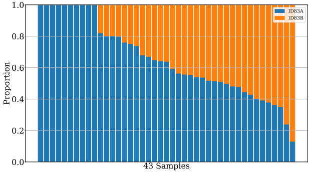

(b) Relative

Figure: Indel Bar Plot in LUAD

Indels in LUAD II

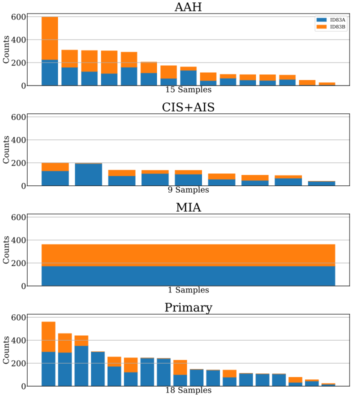

(a) Absolute

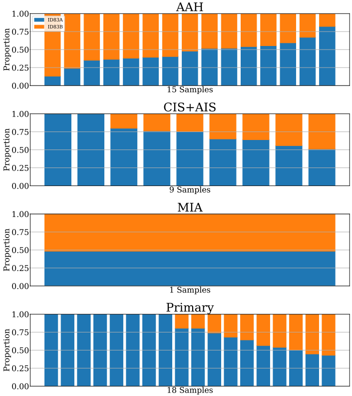

(b) Relative

Figure: Indel Bar Plot by Cancer Subtype in LUAD

Indels in LUAD III

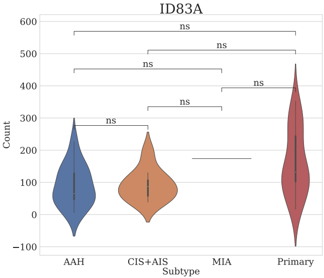

(a) Absolute

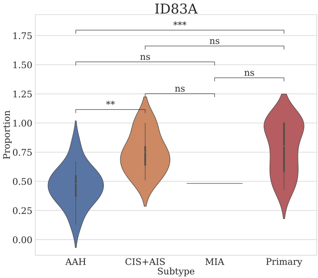

(b) Relative

Figure: Indel83A Signature in LUAD

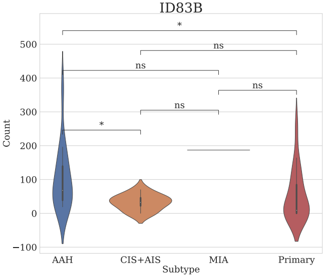

(a) Absolute

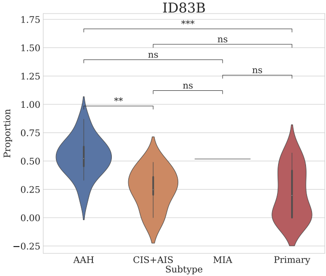

(b) Relative

Figure: Indel83B Signature in LUAD

Indel in LUAD with Smoking

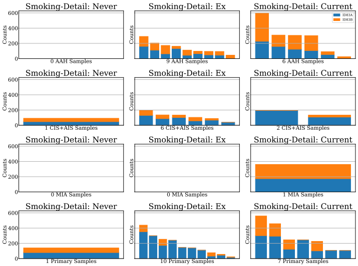

(a) Absolute

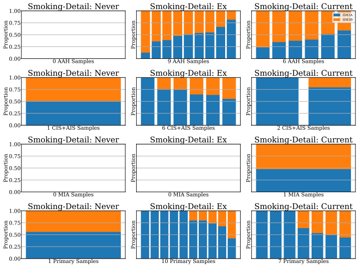

(b) Relative

Figure: Indel Bar Plot by Cancer Subtype & Smoking in LUAD

Indel in LUAD with Recurrence

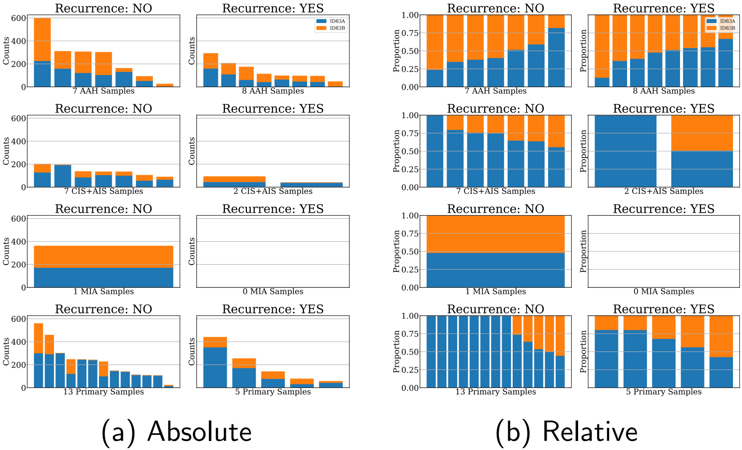

Figure: Indel Bar Plot by Cancer Subtype & Recurrence in LUAD

Findings in Mutation Signature

4. Results

4.9. Clinical Data with Point Mutation

Mutect2?

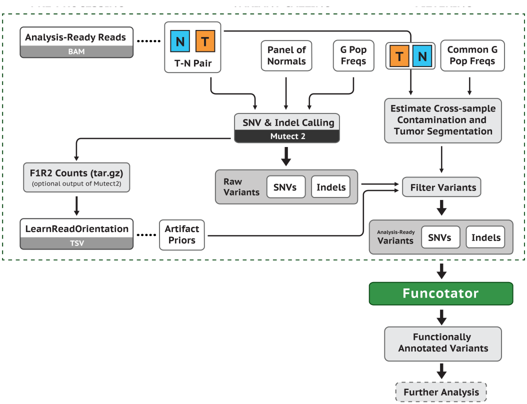

Figure: Somatic short variant discovery workflow (Van der Auwera et al., 2013; DePristo et al., 2011)

4. Results

4.9. Clinical Data with Point Mutation

4.9.1. For Smoking

LUSC with Smoking

Table: LUSC WES Data with Smoking

Smoking?	Stage	Number of Samples
Never	Normal	3
	CIS+AIS	3
	Primary	3
	Total	9
Ex	Normal	41
	Dysplasia	1
	AAH	4
	CIS+AIS	40
	Primary	41
	Total	127
Current	Normal	33
	Dysplasia	4
	AAH	4
	CIS+AIS	30
	Primary	33
	Total	104

Clinical Data about LUSC for Smoking I

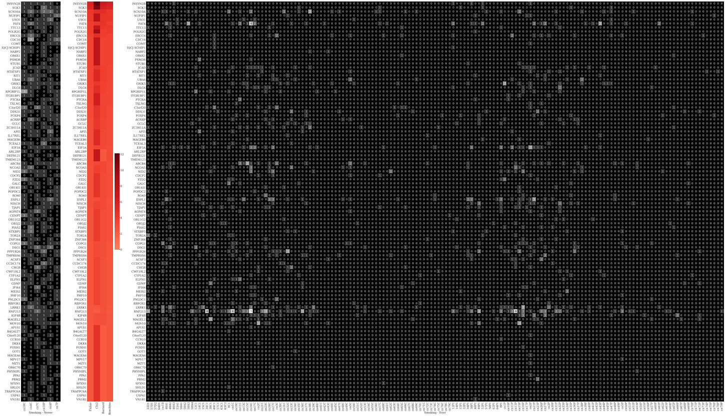

Figure: Clinical Data about LUSC for Smoking

Clinical Data about LUSC for Smoking II

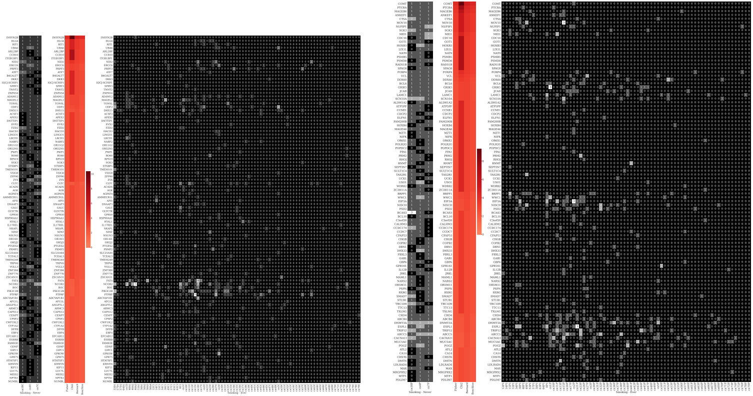

(a) Precancer (b) Primary Cancer

Figure: Clinical Data about LUSC for Smoking with Precancer/Primary

Notable genes in LUSC for Smoking I

INSYN2B

1. INSYN2B is the best indicator for Smoking.
2. INSYN2B is the best indicator for Smoking in Precancer.

COMT

1. COMT is the best indicator for Smoking in Primary.

LUAD with Smoking

Table: LUAD WES Data with Smoking

Smoking?	Stage	Number of Samples
Never	Normal	1
	CIS+AIS	1
	Primary	1
	Total	3
Ex	Normal	10
	AAH	9
	CIS+AIS	6
	Primary	10
	Total	35
Current	Normal	7
	AAH	6
	CIS+AIS	2
	MIA	1
	Primary	7
	Total	23

Clinical Data about LUAD for Smoking I

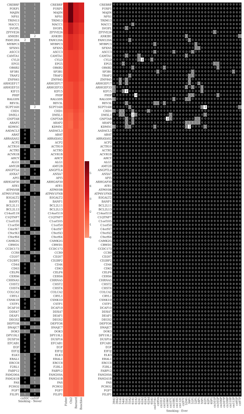

Figure: Clinical Data about LUAD for Smoking

Clinical Data about LUAD for Smoking II

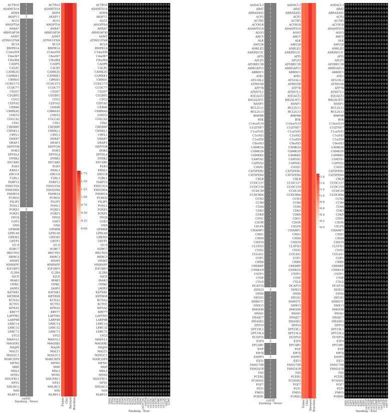

(a) Precancer (b) Primary Cancer

Figure: Clinical Data about LUAD for Smoking with Precancer/Primary

Notable genes in LUAD for Smoking I

CREBRF

1. CREBRF is the best indicator for Smoking.

ACTR10

1. ACTR10 is the best indicator for Smoking in Precancer.

AADACL3

1. AADACL3 is the best indicator for Smoking in Primary.

4. Results

4.9. Clinical Data with Point Mutation

4.9.2. For Recurrence

LUSC with Recurrence

Table: LUSC WES Data with Recurrence

Recurrence?	Stage	Number of Samples
Recurrence	Normal	14
	Dysplasia	4
	CIS+AIS	12
	Primary	14
	Total	44
Non-recurrence	Normal	63
	Dysplasia	1
	AAH	8
	CIS+AIS	61
	Primary	63
	Total	196

Clinical Data about LUSC for Recurrence I

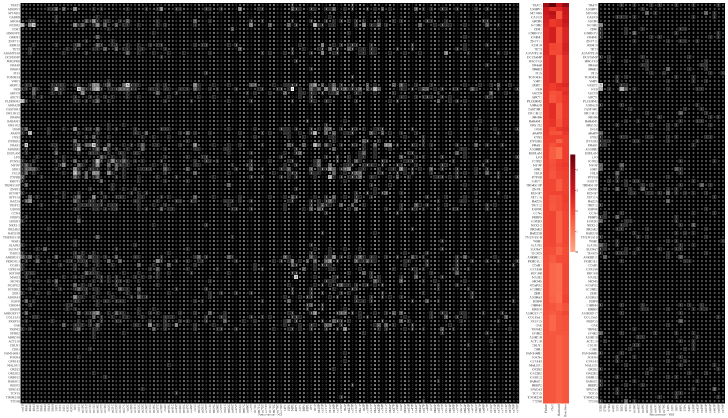

Figure: Clinical Data about LUSC for Recurrence

Clinical Data about LUSC for Recurrence II

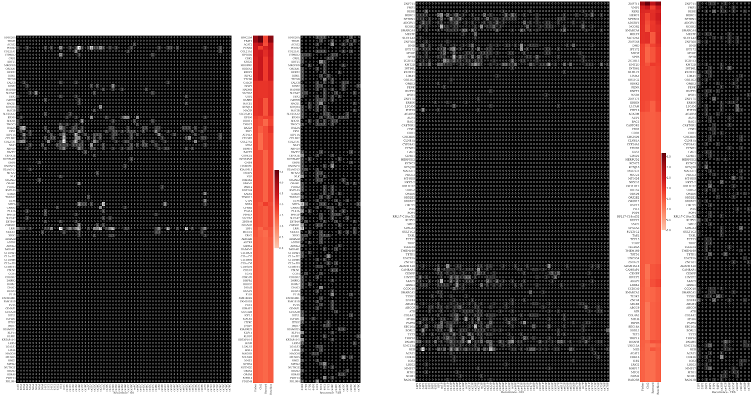

(a) Precancer (b) Primary Cancer

Figure: Clinical Data about LUSC for Recurrence with Precancer/Primary

Notable genes in LUSC with Recurrence I

TRAT1

1. TRAT1 is the best indicator for Recurrence.

HMG20A

1. HMG20A is the best indicator for Recurrence in Precancer.

ZNF711

1. ZNF711 is the best indicator for Recurrence in Primary.

LUAD with Recurrence

Table: LUAD WES Data with Recurrence

Recurrence?	Stage	Number of Samples
Recurrence	Normal	5
	AAH	8
	CIS+AIS	2
	Primary	5
	Total	20
Non-recurrence	Normal	13
	AAH	7
	CIS+AIS	7
	MIA	1
	Primary	13
	Total	41

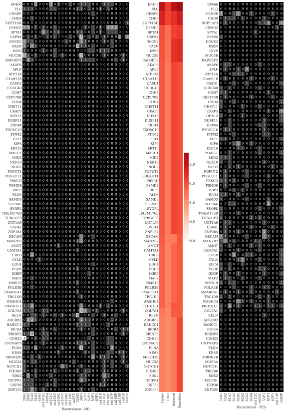

Figure: Clinical Data about LUAD for Recurrence

Clinical Data about LUAD for Recurrence II

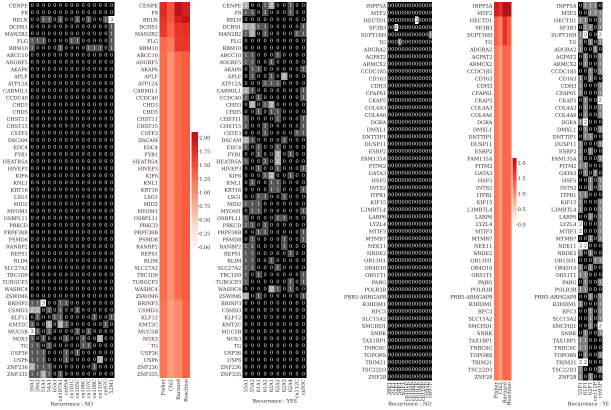

(a) Precancer (b) Primary Cancer

Figure: Clinical Data about LUAD for Recurrence with Precancer/Primary

Notable genes in LUSC with Recurrence I

EP400

1. EP400 is the best indicator for Recurrence.

CENPE

1. CENPE is the best indicator for Recurrence in Precancer.

INPP5A

1. INPP5A is the best indicator for Recurrence in Primary.

Findings in Clinical Data with Point Mutations

4. Results

4.10. Differences in Gene Expression Levels

RSEM?

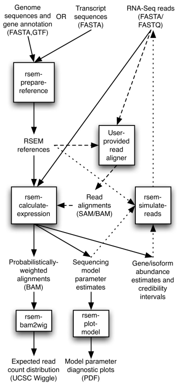

Figure: RSEM workflow (B. Li & Dewey, 2011)

DESeq2?

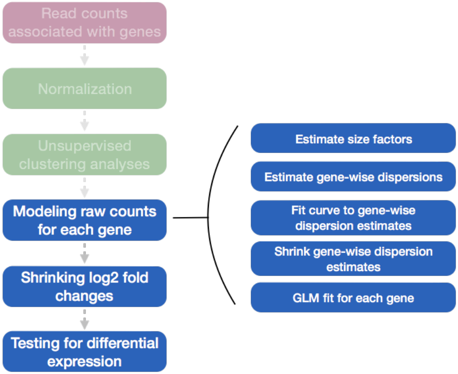

Figure: DESeq2 workflow (Love, Huber, & Anders, 2014)

DEG Selection Strategy

DEG: differentially expressed genes

Fold Change

$\log_2(\text{Fold Change}) > 1 \vee \log_2(\text{Fold Change}) < -1$

P-value

P-value < 0.05

Adjusted P-value

Padj < 0.05

Enrichr?

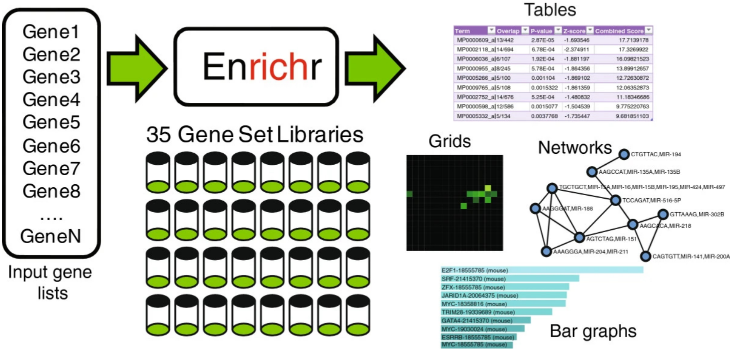

Term	Overlap	P-value	Z-score	Combined Score
MP0000609_a	13/442	2.87E-05	-1.693546	17.7139178
MP0002118_a	14/694	6.78E-04	-2.374911	17.3269922
MP0006036_a	6/107	1.92E-04	-1.881197	16.09821523
MP0000955_a	8/245	5.78E-04	-1.864356	13.89912657
MP0005266_a	5/100	0.001104	-1.869102	12.72630872
MP0009765_a	5/108	0.0015322	-1.861359	12.06352873
MP0002752_a	14/676	5.25E-04	-1.480832	11.18346686
MP0000598_a	12/586	0.0015077	-1.504539	9.775220763
MP0005332_a	5/134	0.0037768	-1.735447	9.681851103

Figure: Enrichr workflow (E. Y. Chen et al., 2013; Kuleshov et al., 2016)

Gene-set Library

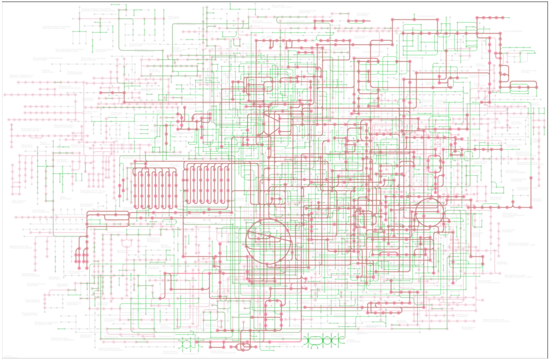

Figure: The global map of metabolic pathways by KEGG (Kanehisa et al., 2021)

KEGG

KEGG 2021 Human

WTS Data Composition

Table: Number of WTS samples

Cancer Subtype	Stage	Number of Samples
LUSC	Normal	17
	Dysplasia	2
	CIS+AIS	34
	Primary	36
	Total	89
LUAD	Normal	13
	AAH	1
	CIS+AIS	5
	Primary	6
	Total	25

WTS Data Composition by Recur I

Table: Number of WTS LUSC samples

Recurrence?	Stage	Number of Samples
Recurrence	Normal	1
	Dysplasia	1
	CIS+AIS	5
	Primary	6
	Total	13
Non-recurrence	Normal	16
	Dysplasia	1
	CIS+AIS	29
	Primary	30
	Total	76

WTS Data Composition by Recur II

Table: Number of WTS LUAD samples

Recurrence?	Stage	Number of Samples
Recurrence	Normal	2
	CIS+AIS	1
	Primary	1
	Total	4
Non-recurrence	Normal	11
	AAH	1
	CIS+AIS	4
	Primary	5
	Total	21

WTS Data Composition by Smoking I

Table: Number of WTS LUSC samples

Smoking?	Stage	Number of Samples
Never	Normal	1
	CIS+AIS	1
	Primary	2
	Total	4
Ex	Normal	8
	Dysplasia	1
	CIS+AIS	21
	Primary	22
	Total	52
Current	Normal	8
	Dysplasia	1
	CIS+AIS	12
	Primary	12
	Total	33

WTS Data Composition by Smoking II

Table: Number of WTS LUAD samples

Smoking?	Stage	Number of Samples
Never	Normal	10
	AAH	1
	CIS+AIS	3
	Primary	4
	Total	18
Ex	Normal	3
	CIS+AIS	1
	Primary	1
	Total	5
Current	CIS+AIS	1
	Primary	1
	Total	2

4. Results

4.10. Differences in Gene Expression Levels

4.10.1. Comparing cancer stage in LUSC

DEG Volcano Plots in LUSC

Normal → Dysplasia → CIS → Primary (LUSC)

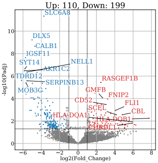

(a) Normal-Dysplasia

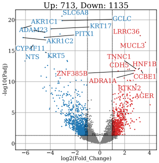

(b) Normal-CIS

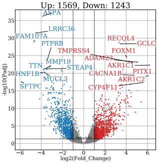

(c) Normal-Primary

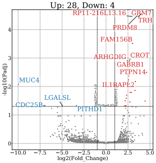

(d) Dysplasia-CIS

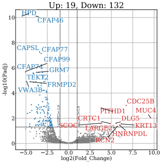

(e) Dysplasia-Primary

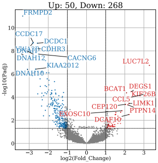

(f) CIS-Primary

Figure: DEG Volcano Plots in LUSC

Normal → Dysplasia → CIS → Primary (LUSC)

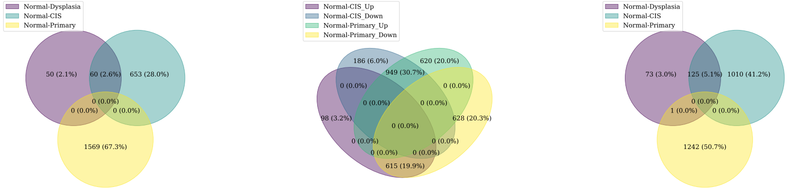

(a) Up-regulated (b) Both (c) Down-regulated

Figure: DEG Venn Diagram in LUSC

Enrichment test with Normal vs. Dysplasia in LUSC

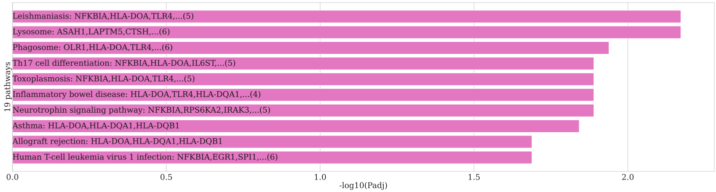

Figure: Up-regulated Pathways on Normal vs. Dysplasia

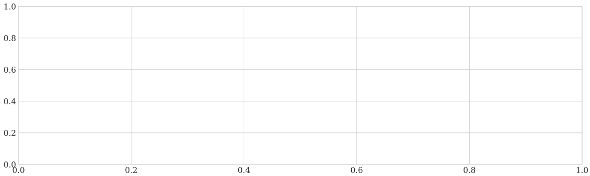

Figure: Down-regulated Pathways on Normal vs. Dysplasia

Enrichment test with Normal vs. CIS in LUSC

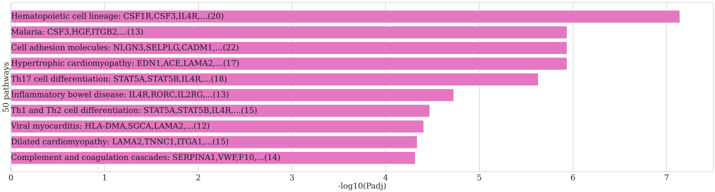

Figure: Up-regulated Pathways on Normal vs. CIS

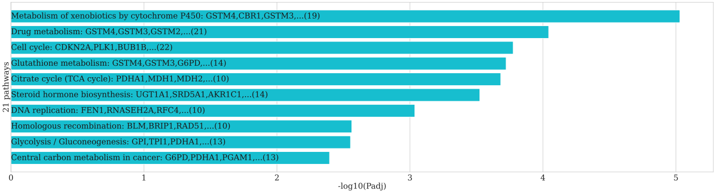

Figure: Down-regulated Pathways on Normal vs. CIS

Enrichment test with Normal vs. Primary in LUSC

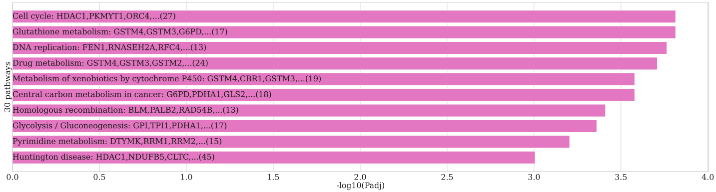

Figure: Up-regulated Pathways on Normal vs. Primary

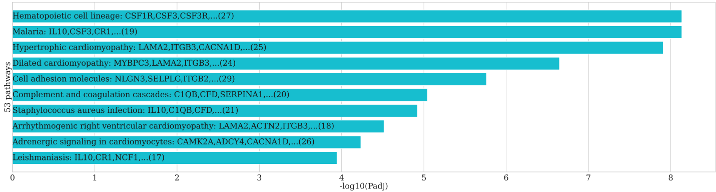

Figure: Down-regulated Pathways on Normal vs. Primary

Findings in Comparing cancer stage in LUSC

AKR1C1 & AKR1C2

1. Down-regulated in CIS, but up-regulated in Primary.
2. Regulate steroids (Jin et al., 2009) and hormones (Penning et al., 2000) .
3. Promote the metastasis of NSCLC (Z. Hong et al., 2018).

SFTPC

1. Down-regulate in Primary than Normal.
2. A pulmonary surfactant associated protein (Z. Lin et al., 2018).
3. SFTPC $\Downarrow \Rightarrow$ Poor survival in LUAD (B. Li et al., 2019).
4. Associated with lung disease in adult (Henderson et al., 2013) and baby (Brasch et al., 2004).

4. Results

4.10. Differences in Gene Expression Levels

4.10.2. Comparing cancer stage in LUAD

DEG Volcano Plots in LUAD

Normal → AAH → AIS → Primary (LUAD)

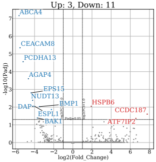

(a) Normal-AAH

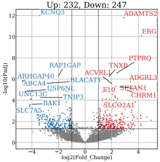

(b) Normal-AIS

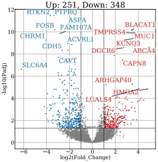

(c) Normal-Primary

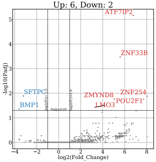

(d) AAH-AIS

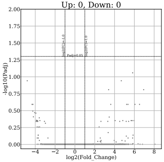

(e) AAH-Primary

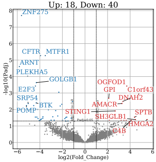

(f) AIS-Primary

Figure: DEG Volcano Plots in LUAD

DEG Venn Diagram in LUAD

Normal $\rightarrow$ AAH $\rightarrow$ AIS $\rightarrow$ Primary (LUAD)

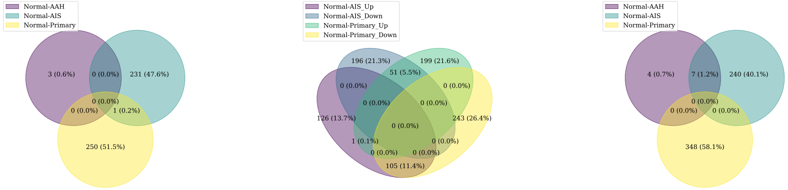

(a) Up-regulated (b) Both (c) Down-regulated

Figure: DEG Venn Diagram in LUAD

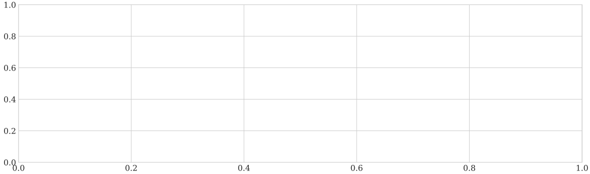

Figure: Up-regulated Pathways on Normal vs. AAH

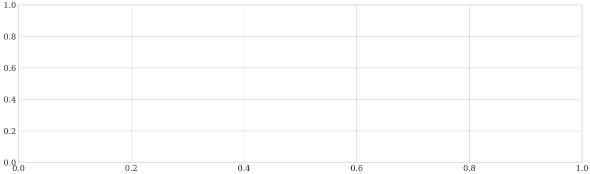

Figure: Down-regulated Pathways on Normal vs. AAH

Enrichment test with Normal vs. AIS in LUAD

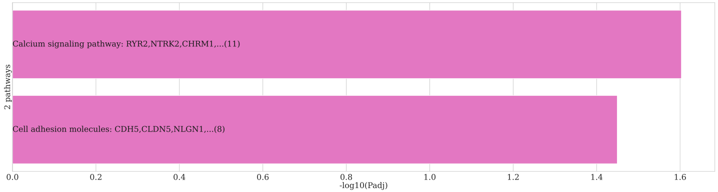

Figure: Up-regulated Pathways on Normal vs. AIS

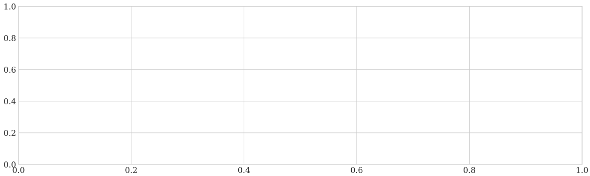

Figure: Down-regulated Pathways on Normal vs. AIS

Enrichment test with Normal vs. Primary in LUAD

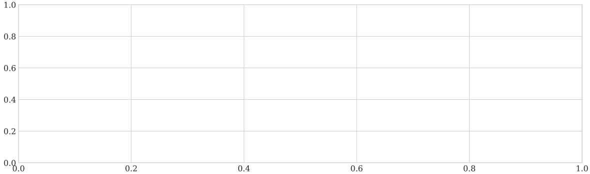

Figure: Up-regulated Pathways on Normal vs. Primary

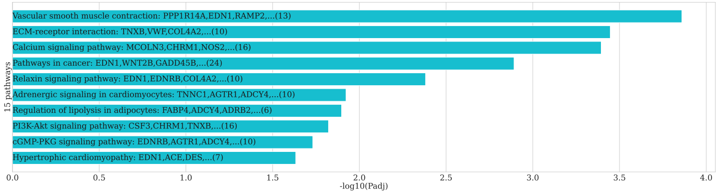

Figure: Down-regulated Pathways on Normal vs. Primary

Finding in Comparing cancer stage in LUAD I

ABCA4

1. Down-regulated in AAH & AIS, but up-regulated in Primary.
2. It is associated with ophthalmology (Maugeri et al., 2000).
3. It shows lung cancer susceptibility in Korean patients (Lee, Lee, Yoon, & Lee, 2013).

Finding in Comparing cancer stage in LUAD II

KCNQ3

1. Down-regulated in AIS, but up-regulated in Primary.
2. K^+ voltage-dependent channels $\Rightarrow$ Various physiological functions (Schroeder, Kubisch, Stein, & Jentsch, 1998; Surti, Huang, Jan, Jan, & Cooper, 2005; Singh et al., 2003).
3. Up-regulated microRNAs in hypoxia-induced LUAD (Geng et al., 2016).
4. KCNQ gene family is associated with lung diseases (Mondejar-Parreño, Perez-Vizcaino, & Cogolludo, 2020).

Finding in Comparing cancer stage in LUAD III

CHRM1

1. Up-regulated in AIS, but down-regulated in Primary.
2. Various cellular responses ⇒ neurodevelopmental disorders (Marcé-Grau et al., 2021), schizophrenia (Dean & Scarr, 2021), and Alzheimer's disease (Counts et al., 2007).
3. Reported down-regulation in LUSC & LUAD (G. Ma et al., 2019).

4. Results

4.10. Differences in Gene Expression Levels

4.10.3. Recur vs. Non-recur in LUSC

LUSC Data Composition

Table: Number of WTS LUSC samples

Recurrence?	Stage	Number of Samples
Recurrence	Normal	1
	Dysplasia	1
	CIS+AIS	5
	Primary	6
	Total	13
Non-recurrence	Normal	16
	Dysplasia	1
	CIS+AIS	29
	Primary	30
	Total	76

Pooled normal samples

In order to compare with Normal stage, merging Normal samples.

$\because$ Insufficient number of Normal samples in Recur.

DEG Volcano Plots for R vs. NR with CIS in LUSC

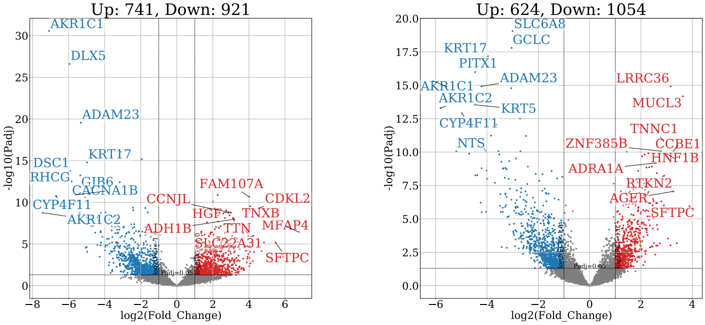

(a) Recur

(b) Non-recur

Figure: DEG Volcanot Plot with CIS in LUSC

DEG Venn Diagram for R vs. NR with CIS in LUSC

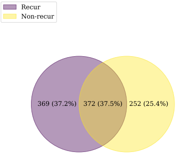

(a) Up-regulated

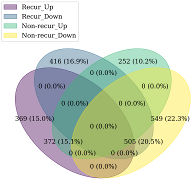

(b) Both

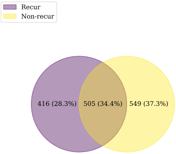

(c) Down-regulated

Figure: DEG Venn Diagram for R vs. NR with CIS in LUSC

Enrichment test for Recur-specific with CIS in LUSC

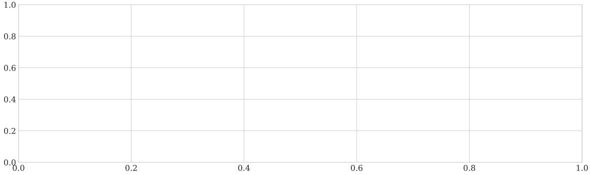

Figure: Up-regulated Pathways for Recur-specific

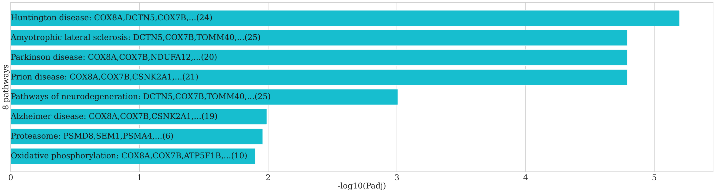

Figure: Down-regulated Pathways for Recur-specific

Enrichment test for Non-recur-specific with CIS in LUSC

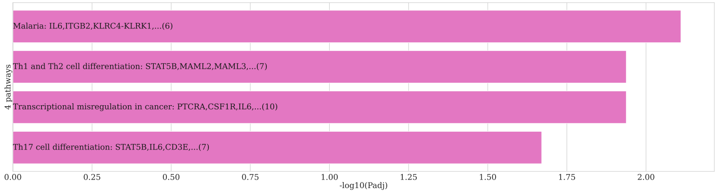

Figure: Up-regulated Pathways for Non-recur-specific

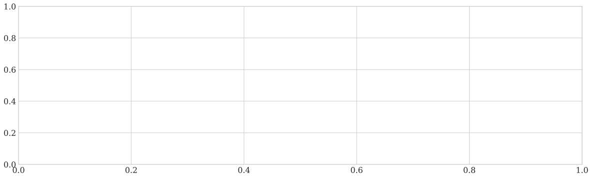

Figure: Down-regulated Pathways for Non-recur-specific

Enrichment test for Intersected with CIS in LUSC

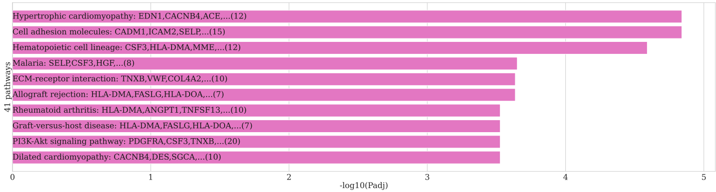

Figure: Up-regulated Pathways for Intersected

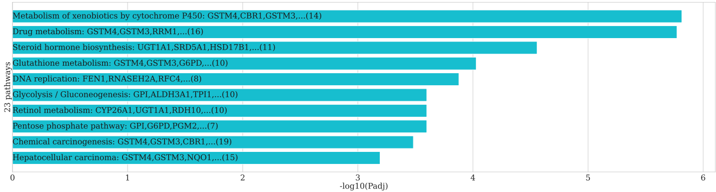

Figure: Down-regulated Pathways for Intersected

DEG Volcano Plots for R vs. NR with Primary in LUSC

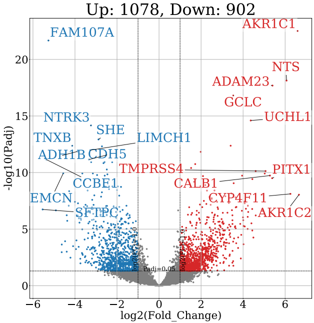

(a) Recur

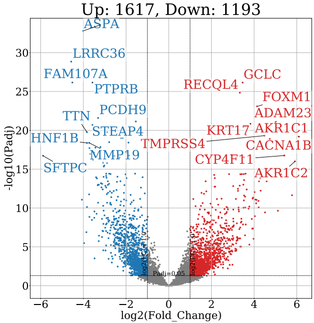

(b) Non-recur

Figure: DEG Volcanot Plot with Primary in LUSC

DEG Venn Diagram for R vs. NR with Primary in LUSC

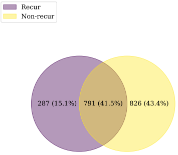

(a) Up-regulated

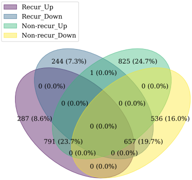

(b) Both

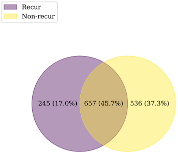

(c) Down-regulated

Figure: DEG Venn Diagram for R vs. NR with Primary in LUSC

Enrichment test for Recur-specific with Primary in LUSC

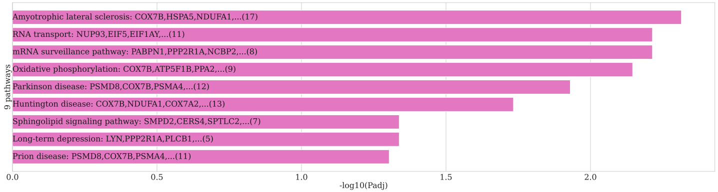

Figure: Up-regulated Pathways for Recur-specific

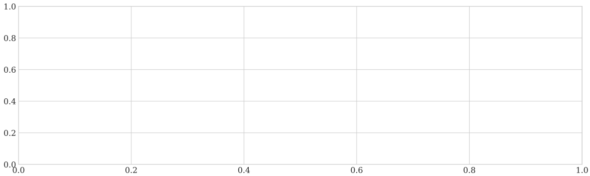

Figure: Down-regulated Pathways for Recur-specific

Enrichment test for NR-specific with Primary in LUSC

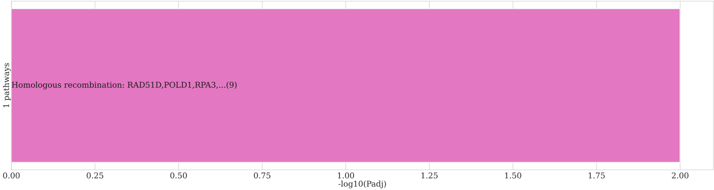

Figure: Up-regulated Pathways for Non-recur-specific

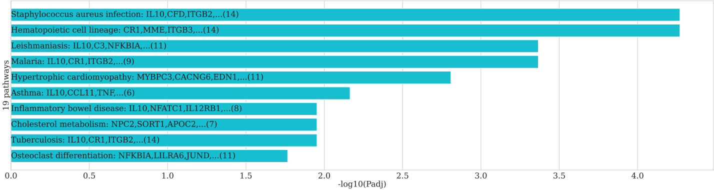

Figure: Down-regulated Pathways for Non-recur-specific

Enrichment test for Intersected with Primary in LUSC

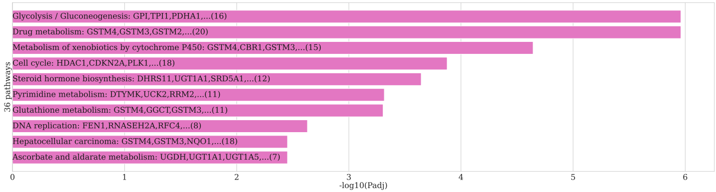

Figure: Up-regulated Pathways for Intersected

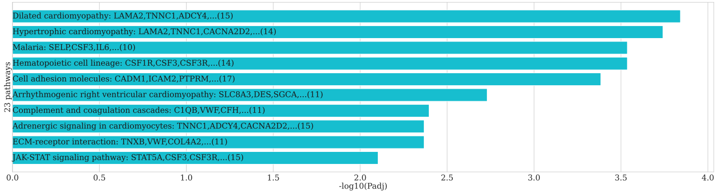

Figure: Down-regulated Pathways for Intersected

Finding in Comparing Recur vs. Non-recur in LUSC I

NTS

1. Highly up-regulated in Recur patients.
2. Neurotensin.
3. Association with non-gastrointestinal cancers (Nikolaou et al., 2020).
4. Modulate lung cancer cell plasticity and heterogeneity (Wu et al., 2019).

NTRK3

1. Highly down-regulated in Recur patients.
2. Activation of NTRK3 in LUSC (Bollig-Fischer et al., 2021).
3. NTRK3 mutation has association with immunotherapy in LUAD (Niu et al., 2020).

Finding in Comparing Recur vs. Non-recur in LUSC II

RECQL4

1. Highly up-regulated in Non-recur patients.
2. DNA-dependent ATPase (Yin, Kwon, Varshavsky, & Wang, 2004)
3. RECQL4 modulate chromosome segregation (Yin et al., 2004)
4. RECQL5 promotes metastasis & resistance in NSCLC (Xia, Zhang, Yuan, & Niu, 2021)
5. RECQL4 $\Uparrow$ $\Rightarrow$ Poor prognosis in breast cancer (X. Zhu et al., 2018)
   1. Overall survival
   2. Distant metastasis-free survival
   3. Relapse-free survival

4. Results

4.10. Differences in Gene Expression Levels

4.10.4. Within Recur in LUSC

DEG Volcano Plots with Recur in LUSC

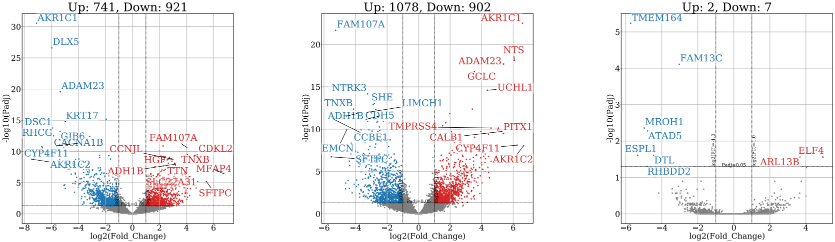

(a) Normal-CIS (b) Normal-Primary (c) CIS-Primary

Figure: DEG Volcano Plots with Recur samples in LUSC

DEG Venn Diagram with Recur in LUSC

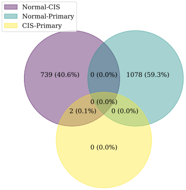

(a) Up-regulated

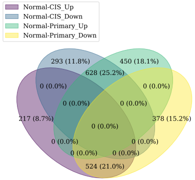

(b) Both

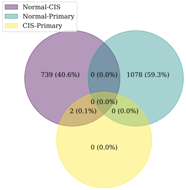

(c) Down-regulated

Figure: DEG Venn Diagram with Recur samples in LUSC

Enrichment test with Normal vs. CIS for Recur

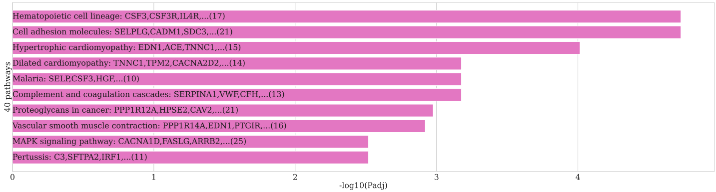

Figure: Up-regulated Pathways on Normal vs. CIS for Recur in LUSC

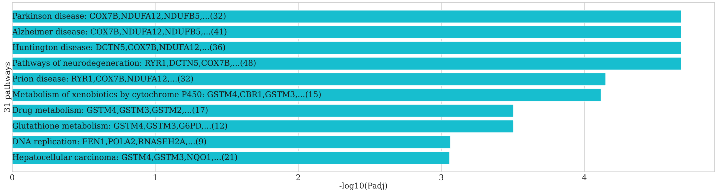

Figure: Down-regulated Pathways on Normal vs. CIS for Recur in LUSC

Enrichment test with Normal vs. Primary for Recur

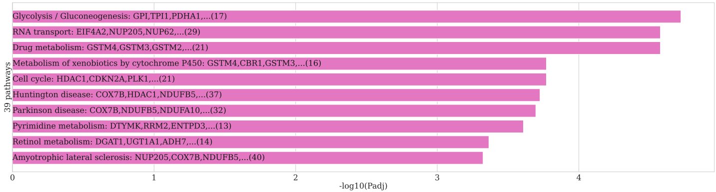

Figure: Up-regulated Pathways on Normal vs. Primary for Recur in LUSC

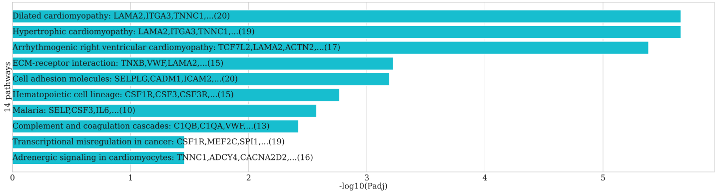

Figure: Down-regulated Pathways on Normal vs. Primary for Recur in LUSC

Finding in Comparing within Recur in LUSC I

AKR1C1

1. Down-regulated in CIS, but up-regulated in Primary.
2. Regulate steroids (Jin et al., 2009) and hormones (Penning et al., 2000).
3. Promote the metastasis of NSCLC (Z. Hong et al., 2018)

ADAM23

1. Down-regulated in CIS, but up-regulated in Primary.
2. Play a role in cell-cell and cell-matrix interactions (Cal, Freije, López, Takada, & Lopez-Otın, 2000)
3. Suppresses metastasis in lung carcinoma cells (Ota et al., 2016)
4. ADAM protein was lower in NSCLC than in normal tissue & benign pulmonary lesions (Hu et al., 2011)

Finding in Comparing within Recur in LUSC II

FAM107A

1. Up-regulated in CIS, but down-regulated in Primary.
2. May play a role in tumor development (L. Wang et al., 2000)
3. Negatively regulates focal adhesion assembly (Le et al., 2010)

4. Results

4.10. Differences in Gene Expression Levels

4.10.5. Within Non-recur in LUSC

DEG Volcano Plots with Non-recur in LUSC

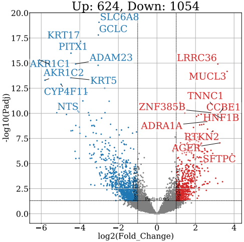

(a) Normal-CIS

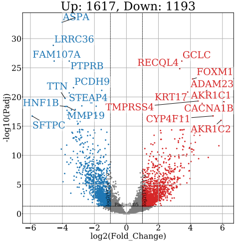

(b) Normal-Primary

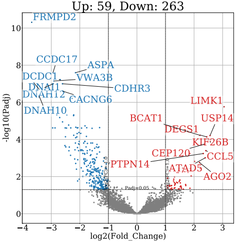

(c) CIS-Primary

Figure: DEG Volcano Plots with Non-recur samples in LUSC

DEG Venn Diagram with Non-recur in LUSC

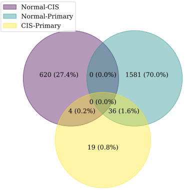

(a) Up-regulated

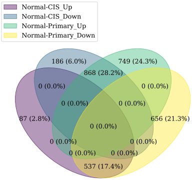

(b) Both

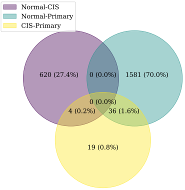

(c) Down-regulated

Figure: DEG Venn Diagram with Non-recur in LUSC

Enrichment test with Normal vs. CIS for Non-recur

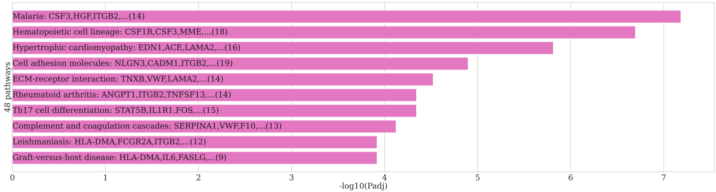

Figure: Up-regulated Pathways on Normal vs. CIS for Non-recur in LUSC

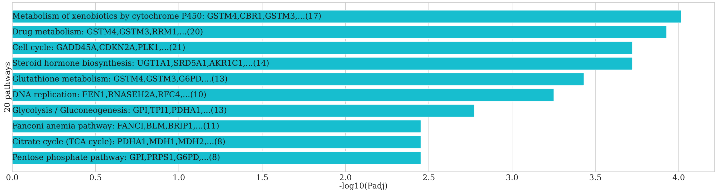

Figure: Down-regulated Pathways on Normal vs. CIS for Non-recur in LUSC

Enrichment test with Normal vs. Primary for Non-recur

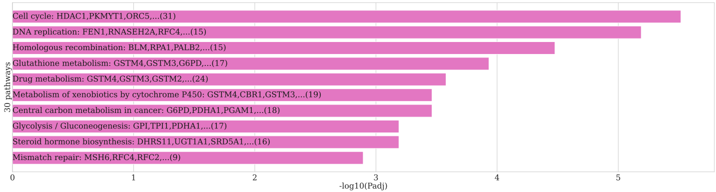

Figure: Up-regulated Pathways on Normal vs. Primary for Non-recur in LUSC

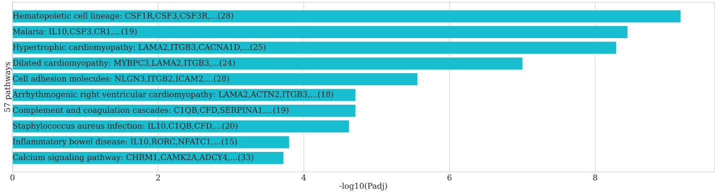

Figure: Down-regulated Pathways on Normal vs. Primary for Non-recur in LUSC

Finding in Comparing within Non-recur in LUSC I

AKR1C1 & AKR1C2

1. Down-regulated in CIS, but up-regulated in Primary.
2. Regulate steroids (Jin et al., 2009) and hormones (Penning et al., 2000)
3. Promote the metastasis of NSCLC (Z. Hong et al., 2018)

CYP4F11

1. Down-regulated in CIS, but up-regulated in Primary.
2. Involved in the metabolism, including fatty acid and their derivatives (Edson et al., 2013; Kalsotra, Turman, Kikuta, & Strobel, 2004; Dhar, Sepkovic, Hirani, Magnusson, & Lasker, 2008)
3. CYP4F11 showed a strong association with survival in colorectal cancer (Alnabulsi, Swan, Cash, Alnabulsi, & Murray, 2017).

Finding in Comparing within Non-recur in LUSC II

LRRC36

1. Up-regulated in CIS, but down-regulated in Primary.
2. Leucine-rich repeat-containing protein 36
3. LRRC36 is positively correlated with survival in LUAD (Zhang et al., 2017).

4. Results

4.10. Differences in Gene Expression Levels

4.10.6. Within Non-recur in LUAD

LUAD Data Composition

Table: Number of WTS LUAD samples

Recurrence?	Stage	Number of Samples
Recurrence	Normal	2
	CIS+AIS	1
	Primary	1
	Total	4
Non-recurrence	Normal	11
	AAH	1
	CIS+AIS	4
	Primary	5
	Total	21

DEG Volcano Plots with Non-recur in LUAD

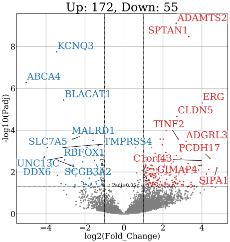

(a) Normal-AIS

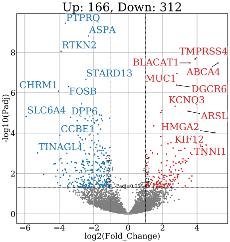

(b) Normal-Primary

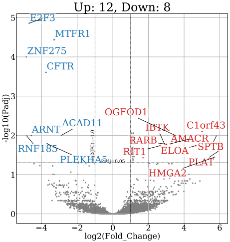

(c) AIS-Primary

Figure: DEG Volcano Plots with Non-recur samples in LUAD

DEG Venn Diagram with Non-recur in LUAD

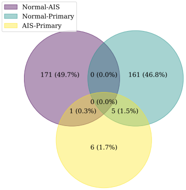

(a) Up-regulated

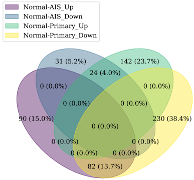

(b) Both

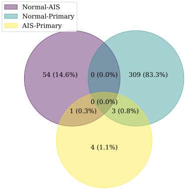

(c) Down-regulated

Figure: DEG Venn Diagram with Non-recur in LUAD

Enrichment test with Normal vs. AIS in LUAD

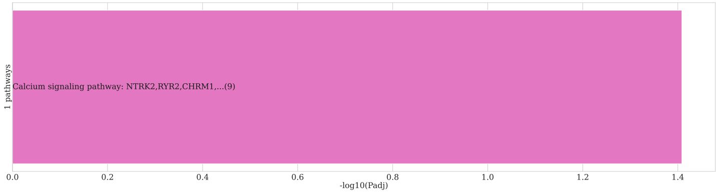

Figure: Up-regulated Pathways on Normal vs. AIS for Non-recur in LUA

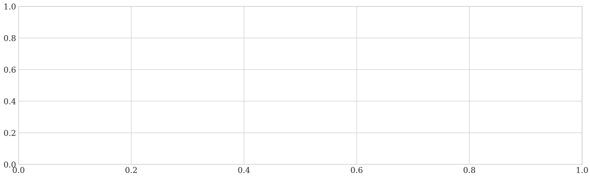

Figure: Down-regulated Pathways on Normal vs. AIS for Non-recur in LUAD

Enrichment test with Normal vs. Primary in LUAD

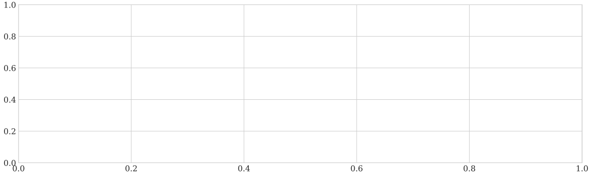

Figure: Up-regulated Pathways on Normal vs. Primary for Non-recur in LUA

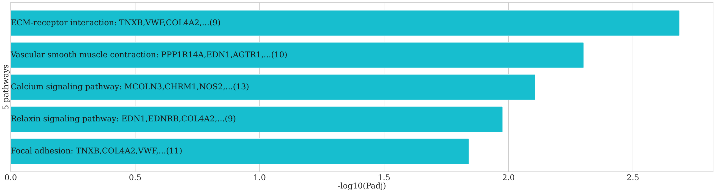

Figure: Down-regulated Pathways on Normal vs. Primary for Non-recur in LUAD

Finding in Comparing within Non-recur in LUAD I

KCNQ3

1. Down-regulated in AIS, but up-regulated in Primary.
2. K^+ voltage-dependent channels $\Rightarrow$ Various physiological functions (Schroeder et al., 1998; Surti et al., 2005; Singh et al., 2003)
3. Up-regulated microRNAs in hypoxia-induced LUAD (Geng et al., 2016)
4. KCNQ gene family is associated with lung diseases (Mondejar-Parreño et al., 2020)

Finding in Comparing within Non-recur in LUAD II

BLACAT1

1. Down-regulated in AIS, but up-regulated in Primary.
2. Bladder cancer-associated transcript 1
3. Chemo-resistance of NSCLC (Huang et al., 2019)
4. Predicts poor prognosis in SCLC (W. Chen et al., 2019)
5. Up-regulated in many human cancers (Ye, Yang, Liu, Lv, & Ye, 2020)

Findings in DEG Analysis

4. Results

4.11. Discovery of Gene Fusion

Arriba?

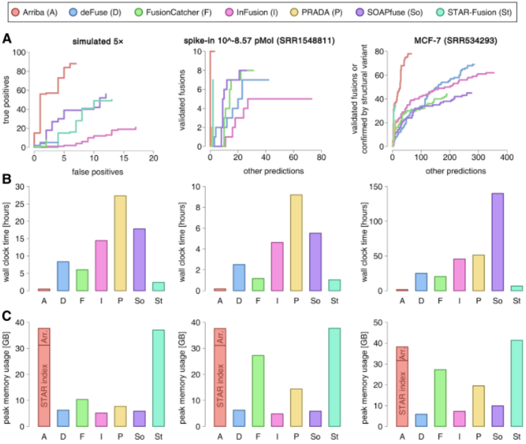

Figure: Benchmark of Arriba versus alternative methods (Uhrig et al., 2021)

Findings in Gene Fusion Discovery

5. Discussion

6. References

Aktaş, O. N., Öztürk, A. B., Erman, B., Erus, S., Tanju, S., & Dilege, Ş. (2018). Role of natural killer cells in lung cancer. *Journal of cancer research and clinical oncology*, *144*(6), 997–1003.

Alexandrov, L. B., Kim, J., Haradhvala, N. J., Huang, M. N., Ng, A. W. T., Wu, Y., ... others (2020). The repertoire of mutational signatures in human cancer. *Nature*, *578*(7793), 94–101.

Alexandrov, L. B., Nik-Zainal, S., Wedge, D. C., Aparicio, S. A., Behjati, S., Biankin, A. V., ... others (2013). Signatures of mutational processes in human cancer. *Nature*, *500*(7463), 415–421.

Alnabulsi, A., Swan, R., Cash, B., Alnabulsi, A., & Murray, G. I. (2017). The differential expression of omega-3 and omega-6 fatty acid metabolising enzymes in colorectal cancer and its prognostic significance. *British journal of cancer*, *116*(12), 1612–1620.

References II

Andrews, S., Krueger, F., Segonds-Pichon, A., Biggins, L., Krueger, C., & Wingett, S. (2012, January). *FastQC.* Babraham Institute. Babraham, UK.

Behrend, S. J., Giotopoulou, G. A., Spella, M., & Stathopoulos, G. T. (2021). A role for club cells in smoking-associated lung adenocarcinoma. *European Respiratory Review*, *30*(162).

Bergstrom, E. N., Barnes, M., Martincorena, I., & Alexandrov, L. B. (2020). Generating realistic null hypothesis of cancer mutational landscapes using sigprofilersimulator. *BMC bioinformatics*, *21*(1), 1–10.

Bergstrom, E. N., Huang, M. N., Mahto, U., Barnes, M., Stratton, M. R., Rozen, S. G., & Alexandrov, L. B. (2019). Sigprofilermatrixgenerator: a tool for visualizing and exploring patterns of small mutational events. *BMC genomics*, *20*(1), 1–12.

References III

Bernimoulin, M. P., Zeng, X.-L., Abbal, C., Giraud, S., Martinez, M., Michielin, O., . . . Spertini, O. (2003). Molecular basis of leukocyte rolling on psgl-1: predominant role of core-2 o-glycans and of tyrosine sulfate residue 51. *Journal of Biological Chemistry*, *278*(1), 37–47.

Beyer, M., & Schultze, J. L. (2006). Regulatory t cells in cancer. *Blood*, *108*(3), 804–811.

Bollig-Fischer, A., Bao, B., Manning, M., Dyson, G., Michelhaugh, S. K., Mittal, S., . . . Mamdani, H. (2021). Role of novel cancer gene slitrk3 to activate ntrk3 in squamous cell lung cancer. *Molecular Biomedicine*, *2*(1), 1–12.

Brahimi-Horn, M. C., Chiche, J., & Pouysségur, J. (2007). Hypoxia and cancer. *Journal of molecular medicine*, *85*(12), 1301–1307.

Brasch, F., Griese, M., Tredano, M., Johnen, G., Ochs, M., Rieger, C., ... Beers, M. (2004). Interstitial lung disease in a baby with a de novo mutation in the sftpc gene. *European Respiratory Journal*, *24*(1), 30–39.

Cailhier, J. F., Sawatzky, D. A., Kipari, T., Houlberg, K., Walbaum, D., Watson, S., ... others (2006). Resident pleural macrophages are key orchestrators of neutrophil recruitment in pleural inflammation. *American journal of respiratory and critical care medicine*, *173*(5), 540–547.

Cal, S., Freije, J. M., López, J. M., Takada, Y., & Lopez-Otın, C. (2000). Adam 23/mdc3, a human disintegrin that promotes cell adhesion via interaction with the αvβ3 integrin through an rgd-independent mechanism. *Molecular biology of the cell*, *11*(4), 1457–1469.

References V

Chen, E. Y., Tan, C. M., Kou, Y., Duan, Q., Wang, Z., Meirelles, G. V., . . . Ma'ayan, A. (2013). Enrichr: interactive and collaborative html5 gene list enrichment analysis tool. *BMC bioinformatics*, *14*(1), 1–14.

Chen, J.-M., Férec, C., & Cooper, D. N. (2013). Patterns and mutational signatures of tandem base substitutions causing human inherited disease. *Human mutation*, *34*(8), 1119–1130.

Chen, W., Hang, Y., Xu, W., Wu, J., Chen, L., Chen, J., . . . Wang, H. (2019). Blacat1 predicts poor prognosis and serves as oncogenic lncrna in small-cell lung cancer. *Journal of cellular biochemistry*, *120*(2), 2540–2546.

Choi, B., Han, T.-S., Min, J., Hur, K., Lee, S.-M., Lee, H.-J., . . . Yang, H.-K. (2017). Mal and tmem220 are novel dna methylation markers in human gastric cancer. *Biomarkers*, *22*(1), 35–44.

References VI

Collins, L. G., Haines, C., Perkel, R., & Enck, R. E. (2007). Lung cancer: diagnosis and management. *American family physician*, *75*(1), 56–63.

Counts, S. E., He, B., Che, S., Ikonomovic, M. D., DeKosky, S. T., Ginsberg, S. D., & Mufson, E. J. (2007). α7 nicotinic receptor up-regulation in cholinergic basal forebrain neurons in alzheimer disease. *Archives of neurology*, *64*(12), 1771–1776.

Crowdis, J., He, M. X., Reardon, B., & Van Allen, E. M. (2020). Comut: visualizing integrated molecular information with comutation plots. *Bioinformatics*, *36*(15), 4348–4349.

Dean, B., & Scarr, E. (2021). Changes in cortical gene expression in the muscarinic m1 receptor knockout mouse: potential relevance to schizophrenia, alzheimer's disease and cognition. *npj Schizophrenia*, *7*(1), 1–7.

References VII

Deckers, J., Hammad, H., & Hoste, E. (2018). Langerhans cells: sensing the environment in health and disease. *Frontiers in immunology*, *9*, 93.

de Marco, M. C., Martín-Belmonte, F., Kremer, L., Albar, J. P., Correas, I., Vaerman, J. P., ... Alonso, M. A. (2002). Mal2, a novel raft protein of the mal family, is an essential component of the machinery for transcytosis in hepatoma hepg2 cells. *Journal of Cell Biology*, *159*(1), 37–44.

DePristo, M. A., Banks, E., Poplin, R., Garimella, K. V., Maguire, J. R., Hartl, C., ... others (2011). A framework for variation discovery and genotyping using next-generation dna sequencing data. *Nature genetics*, *43*(5), 491.

Dhar, M., Sepkovic, D. W., Hirani, V., Magnusson, R. P., & Lasker, J. M. (2008). Omega oxidation of 3-hydroxy fatty acids by the human cyp4f gene subfamily enzyme cyp4f11. *Journal of lipid research*, *49*(3), 612–624.

Ding, L., Ley, T. J., Larson, D. E., Miller, C. A., Koboldt, D. C., Welch, J. S., . . . others (2012). Clonal evolution in relapsed acute myeloid leukaemia revealed by whole-genome sequencing. *Nature*, *481*(7382), 506–510.

Dosenbach, N. U., Fair, D. A., Miezin, F. M., Cohen, A. L., Wenger, K. K., Dosenbach, R. A., . . . others (2007). Distinct brain networks for adaptive and stable task control in humans. *Proceedings of the National Academy of Sciences*, *104*(26), 11073–11078.

References IX

Duhig, E., Clarke, B., Yang, I. A., Fong, K. M., Hunter, L., Windsor, M., . . . others (2014). Comprehensive molecular profiling of lung adenocarcinoma: the cancer genome atlas research network. *Nature*, *511*(7511), 543–550.

Edson, K. Z., Prasad, B., Unadkat, J. D., Suhara, Y., Okano, T., Guengerich, F. P., & Rettie, A. E. (2013). Cytochrome p450-dependent catabolism of vitamin k: ω-hydroxylation catalyzed by human cyp4f2 and cyp4f11. *Biochemistry*, *52*(46), 8276–8285.

Erfani, N., Mehrabadi, S. M., Ghayumi, M. A., Haghshenas, M. R., Mojtahedi, Z., Ghaderi, A., & Amani, D. (2012). Increase of regulatory t cells in metastatic stage and ctla-4 over expression in lymphocytes of patients with non-small cell lung cancer (nsclc). *Lung cancer*, *77*(2), 306–311.

References X

Geng, Y., Deng, L., Su, D., Xiao, J., Ge, D., Bao, Y., & Jing, H. (2016). Identification of crucial micrornas and genes in hypoxia-induced human lung adenocarcinoma cells. *OncoTargets and therapy*, *9*, 4605.

Goldstraw, P., Ball, D., Jett, J. R., Le Chevalier, T., Lim, E., Nicholson, A. G., & Shepherd, F. A. (2011). Non-small-cell lung cancer. *The Lancet*, *378*(9804), 1727–1740.

Goveia, J., Rohlenova, K., Taverna, F., Treps, L., Conradi, L.-C., Pircher, A., . . . others (2020). An integrated gene expression landscape profiling approach to identify lung tumor endothelial cell heterogeneity and angiogenic candidates. *Cancer cell*, *37*(1), 21–36.

Greczmiel, U., Kräutler, N. J., Pedrioli, A., Bartsch, I., Agnellini, P., Bedenikovic, G., . . . Oxenius, A. (2017). Sustained t follicular helper cell response is essential for control of chronic viral infection. *Science Immunology*, *2*(18).

References XI

Gridelli, C., Rossi, A., Carbone, D. P., Guarize, J., Karachaliou, N., Mok, T., ... Rosell, R. (2015). Non-small-cell lung cancer. *Nature reviews Disease primers*, *1*(1), 1–16.

Grzegrzolka, J., Olbromski, M., Gomulkiewicz, A., Piotrowska, A., Glatzel-Plucinska, N., Ratajczak, K., ... others (2021). Role of tesmin expression in non-small cell lung cancer. *Oncology Letters*, *21*(1), 1–1.

Gueguen, P., Metoikidou, C., Dupic, T., Lawand, M., Goudot, C., Baulande, S., ... others (2021). Contribution of resident and circulating precursors to tumor-infiltrating cd8+ t cell populations in lung cancer. *Science Immunology*, *6*(55), eabd5778.

Henderson, L. B., Melton, K., Wert, S., Couriel, J., Bush, A., Ashworth, M., & Nogee, L. M. (2013). Large abca3 and sftpc deletions resulting in lung disease. *Annals of the American Thoracic Society*, *10*(6), 602–607.

Hong, S., Won, Y.-J., Lee, J. J., Jung, K.-W., Kong, H.-J., Im, J.-S., . . . others (2021). Cancer statistics in korea: Incidence, mortality, survival, and prevalence in 2018. *Cancer Research and Treatment: Official Journal of Korean Cancer Association*, *53*(2), 301.

Hong, Z., Chang, L.-L., Fang-Jie, Y., Yan, H., Chen-Ming, Z., Tian-Yi, Z., . . . others (2018). Akr1c1 activates stat3 to promote the metastasis of non-small cell lung cancer. *Theranostics*, *8*(3), 676.

Hu, C., Lv, H., Pan, G., Cao, H., Deng, Z., Hu, C., . . . Zhou, J. (2011). The expression of adam23 and its correlation with promoter methylation in non-small-cell lung carcinoma. *International journal of experimental pathology*, *92*(5), 333–339.

Huang, F.-X., Chen, H.-J., Zheng, F.-X., Gao, Z.-Y., Sun, P.-F., Peng, Q., . . . others (2019). Lncrna blacat1 is involved in chemoresistance of non-small cell lung cancer cells by regulating autophagy. *International journal of oncology*, *54*(1), 339–347.

Islam, S. M. A., Wu, Y., Díaz-Gay, M., Bergstrom, E. N., He, Y., Barnes, M., . . . Alexandrov, L. B. (2021). Uncovering novel mutational signatures by de novo extraction with sigprofilerextractor. *bioRxiv*. Retrieved from https://www.biorxiv.org/content/early/2021/05/16/2020.12.13.422570 doi: 10.1101/2020.12.13.422570

Jew, B., Alvarez, M., Rahmani, E., Miao, Z., Ko, A., Garske, K. M., . . . Halperin, E. (2020). Accurate estimation of cell composition in bulk expression through robust integration of single-cell information. *Nature communications*, *11*(1), 1–11.

Jin, Y., Duan, L., Lee, S. H., Kloosterboer, H. J., Blair, I. A., & Penning, T. M. (2009). Human cytosolic hydroxysteroid dehydrogenases of the aldo-ketoreductase superfamily catalyze reduction of conjugated steroids. *Journal of Biological Chemistry*, *284*(15), 10013–10022.

References XIV

Kalsotra, A., Turman, C. M., Kikuta, Y., & Strobel, H. W. (2004). Expression and characterization of human cytochrome p450 4f11: Putative role in the metabolism of therapeutic drugs and eicosanoids. *Toxicology and applied pharmacology*, *199*(3), 295–304.

Kanehisa, M., Furumichi, M., Sato, Y., Ishiguro-Watanabe, M., & Tanabe, M. (2021). Kegg: integrating viruses and cellular organisms. *Nucleic acids research*, *49*(D1), D545–D551.

Kim, E. Y., Cha, Y. J., Lee, S. H., Jeong, S., Choi, Y. J., Moon, D. H., . . . Chang, Y. S. (2022). Early lung carcinogenesis and tumor microenvironment observed by single-cell transcriptome analysis. *Translational oncology*, *15*(1), 101277.

Kim, N., Kim, H. K., Lee, K., Hong, Y., Cho, J. H., Choi, J. W., . . . others (2020). Single-cell rna sequencing demonstrates the molecular and cellular reprogramming of metastatic lung adenocarcinoma. *Nature communications*, *11*(1), 1–15.

References XV

Kou, F., Sun, H., Wu, L., Li, B., Zhang, B., Wang, X., & Yang, L. (2020). Top2a promotes lung adenocarcinoma cells' malignant progression and predicts poor prognosis in lung adenocarcinoma. *Journal of Cancer*, *11*(9), 2496.

Kuleshov, M. V., Jones, M. R., Rouillard, A. D., Fernandez, N. F., Duan, Q., Wang, Z., ... others (2016). Enrichr: a comprehensive gene set enrichment analysis web server 2016 update. *Nucleic acids research*, *44*(W1), W90–W97.

Kumari, S., Arora, M., Singh, J., Chauhan, S. S., Kumar, S., & Chopra, A. (2021). L-selectin expression is associated with inflammatory microenvironment and favourable prognosis in breast cancer. *3 Biotech*, *11*(2), 1–13.

Kyotani, Y., Takasawa, S., & Yoshizumi, M. (2019). Proliferative pathways of vascular smooth muscle cells in response to intermittent hypoxia. *International journal of molecular sciences*, *20*(11), 2706.

References XVI

Lara-Lemus, R. (2019). On the role of myelin and lymphocyte protein (mal) in cancer: a puzzle with two faces. *Journal of Cancer*, *10*(10), 2312.

Le, P., Angers-Loustau, A., De Oliveira, R., Ajlan, A., Brassard, C., Dudley, A., . . . others (2010). Drr drives brain cancer invasion by regulating cytoskeletal-focal adhesion dynamics. *Oncogene*, *29*(33), 4636–4647.

Lee, D., Lee, G. K., Yoon, K.-A., & Lee, J. S. (2013). Pathway-based analysis using genome-wide association data from a korean non-small cell lung cancer study. *PloS one*, *8*(6), e65396.

Li, B., Brady, S. W., Ma, X., Shen, S., Zhang, Y., Li, Y., . . . others (2020). Therapy-induced mutations drive the genomic landscape of relapsed acute lymphoblastic leukemia. *Blood*, *135*(1), 41–55.

Li, B., & Dewey, C. N. (2011). Rsem: accurate transcript quantification from rna-seq data with or without a reference genome. *BMC bioinformatics*, *12*(1), 1–16.

Li, B., Meng, Y.-Q., Li, Z., Yin, C., Lin, J.-P., Zhu, D.-J., & Zhang, S.-B. (2019). Mir-629-3p-induced downregulation of sftpc promotes cell proliferation and predicts poor survival in lung adenocarcinoma. *Artificial cells, nanomedicine, and biotechnology*, *47*(1), 3286–3296.

Li, D., Zhang, J., Wu, L., Yang, X., Chen, Z., & Yuan, J. (2021). Myelin and lymphocyte protein (mal): A novel biomarker for uterine corpus endometrial carcinoma. *Cancer Management and Research*, *13*, 7311.

Lin, C., Song, H., Huang, C., Yao, E., Gacayan, R., Xu, S.-M., & Chuang, P.-T. (2012). Alveolar type ii cells possess the capability of initiating lung tumor development. *PloS one*, *7*(12), e53817.

Lin, Z., Thorenoor, N., Wu, R., DiAngelo, S. L., Ye, M., Thomas, N. J., . . . Floros, J. (2018). Genetic association of pulmonary surfactant protein genes, sftpa1, sftpa2, sftpb, sftpc, and sftpd with cystic fibrosis. *Frontiers in immunology*, *9*, 2256.

Liu, X., Xu, X., Deng, W., Huang, M., Wu, Y., Zhou, Z., . . . others (2019). Ccl18 enhances migration, invasion and emt by binding ccr8 in bladder cancer cells. *Molecular medicine reports*, *19*(3), 1678–1686.

Liu, Y.-Z., Wang, B.-S., Jiang, Y.-Y., Cao, J., Hao, J.-J., Zhang, Y., . . . Wang, M.-R. (2017). Mcms expression in lung cancer: implication of prognostic significance. *Journal of Cancer*, *8*(18), 3641.

Love, M. I., Huber, W., & Anders, S. (2014). Moderated estimation of fold change and dispersion for rna-seq data with deseq2. *Genome biology*, *15*(12), 1–21.

Ma, G., Ji, D., Qu, X., Liu, S., Yang, X., Wang, G., ... Du, J. (2019). Mining and validating the expression pattern and prognostic value of acetylcholine receptors in non-small cell lung cancer. *Medicine*, *98*(20).

Ma, W., Wang, B., Zhang, Y., Wang, Z., Niu, D., Chen, S., ... others (2019). Prognostic significance of top2a in non-small cell lung cancer revealed by bioinformatic analysis. *Cancer cell international*, *19*(1), 1–17.

Marcé-Grau, A., Elorza-Vidal, X., Pérez-Rius, C., Ruiz-Nel· lo, A., Sala-Coromina, J., Gabau, E., ... Macaya, A. (2021). Muscarinic acetylcholine receptor m1 mutations causing neurodevelopmental disorder and epilepsy. *Human Mutation*.

Mason, R. J. (2006). Biology of alveolar type ii cells. *Respirology*, *11*, S12–S15.

References XX

Maugeri, A., Klevering, B. J., Rohrschneider, K., Blankenagel, A., Brunner, H. G., Deutman, A. F., . . . Cremers, F. P. (2000). Mutations in the abca4 (abcr) gene are the major cause of autosomal recessive cone-rod dystrophy. *The American Journal of Human Genetics*, *67*(4), 960–966.

Mermel, C. H., Schumacher, S. E., Hill, B., Meyerson, M. L., Beroukhim, R., & Getz, G. (2011). Gistic2. 0 facilitates sensitive and confident localization of the targets of focal somatic copy-number alteration in human cancers. *Genome biology*, *12*(4), 1–14.

Minna, J. D., Roth, J. A., & Gazdar, A. F. (2002). Focus on lung cancer. *Cancer cell*, *1*(1), 49–52.

Modi, B. G., Neustadter, J., Binda, E., Lewis, J., Filler, R. B., Roberts, S. J., . . . others (2012). Langerhans cells facilitate epithelial dna damage and squamous cell carcinoma. *Science*, *335*(6064), 104–108.

References XXI

Mondejar-Parreño, G., Perez-Vizcaino, F., & Cogolludo, A. (2020). Kv7 channels in lung diseases. *Frontiers in Physiology*, *11*, 634.

Nikolaou, S., Qiu, S., Fiorentino, F., Simillis, C., Rasheed, S., Tekkis, P., & Kontovounisios, C. (2020). The role of neurotensin and its receptors in non-gastrointestinal cancers: a review. *Cell Communication and Signaling*, *18*(1), 1–10.

Nik-Zainal, S., Alexandrov, L. B., Wedge, D. C., Van Loo, P., Greenman, C. D., Raine, K., ... others (2012a). Mutational processes molding the genomes of 21 breast cancers. *Cell*, *149*(5), 979–993.

Nik-Zainal, S., Alexandrov, L. B., Wedge, D. C., Van Loo, P., Greenman, C. D., Raine, K., ... others (2012b). Mutational processes molding the genomes of 21 breast cancers. *Cell*, *149*(5), 979–993.

References XXII

Niu, Y., Lin, A., Luo, P., Zhu, W., Wei, T., Tang, R., ... Zhang, J. (2020). Prognosis of lung adenocarcinoma patients with ntrk3 mutations to immune checkpoint inhibitors. *Frontiers in pharmacology*, *11*, 1213.

Olingy, C. E., Dinh, H. Q., & Hedrick, C. C. (2019). Monocyte heterogeneity and functions in cancer. *Journal of leukocyte biology*, *106*(2), 309–322.

Ota, M., Mochizuki, S., Shimoda, M., Abe, H., Miyamae, Y., Ishii, K., ... Okada, Y. (2016). Adam 23 is downregulated in side population and suppresses lung metastasis of lung carcinoma cells. *Cancer science*, *107*(4), 433–443.

Paul, R., Hu, B., Musahl, C., Hameister, H., & Knippers, R. (1996). Coding sequence and chromosome mapping of the human gene (cdc46) for replication protein hcdc46/mcm5. *Cytogenetic and Genome Research*, *73*(4), 317–321.

Penning, T. M., Burczynski, M. E., Jez, J. M., Hung, C.-F., Lin, H.-K., Ma, H., … RATNAM, K. (2000). Human 3α-hydroxysteroid dehydrogenase isoforms (akr1c1–akr1c4) of the aldo-keto reductase superfamily: functional plasticity and tissue distribution reveals roles in the inactivation and formation of male and female sex hormones. *Biochemical journal*, *351*(1), 67–77.

Pinto, A., Rega, A., Crother, T. R., & Sorrentino, R. (2012). Plasmacytoid dendritic cells and their therapeutic activity in cancer. *Oncoimmunology*, *1*(5), 726–734.

Plitas, G., Konopacki, C., Wu, K., Bos, P. D., Morrow, M., Putintseva, E. V., … Rudensky, A. Y. (2016). Regulatory t cells exhibit distinct features in human breast cancer. *Immunity*, *45*(5), 1122–1134.

Poonia, B., Ayithan, N., Nandi, M., Masur, H., & Kottilil, S. (2018a). Hbv induces inhibitory fcrl receptor on b cells and dysregulates b cell-t follicular helper cell axis. *Scientific reports*, *8*(1), 1–14.

References XXIV

Poonia, B., Ayithan, N., Nandi, M., Masur, H., & Kottilil, S. (2018b). Hbv induces inhibitory fcrl receptor on b cells and dysregulates b cell-t follicular helper cell axis. *Scientific reports*, *8*(1), 1–14.

Rawlins, E. L., & Hogan, B. L. (2008). Ciliated epithelial cell lifespan in the mouse trachea and lung. *American Journal of Physiology-Lung Cellular and Molecular Physiology*, *295*(1), L231–L234.

Riester, M., Singh, A. P., Brannon, A. R., Yu, K., Campbell, C. D., Chiang, D. Y., & Morrissey, M. P. (2016). Purecn: copy number calling and snv classification using targeted short read sequencing. *Source code for biology and medicine*, *11*(1), 1–13.

Rokicki, W., Rokicki, M., Wojtacha, J., & Dżeljijli, A. (2016). The role and importance of club cells (clara cells) in the pathogenesis of some respiratory diseases. *Kardiochirurgia i torakochirurgia polska= Polish journal of cardio-thoracic surgery*, *13*(1), 26.

Roth, A., Khattra, J., Yap, D., Wan, A., Laks, E., Biele, J., . . . Shah, S. P. (2014). Pyclone: statistical inference of clonal population structure in cancer. *Nature methods*, *11*(4), 396–398.

Salamon, P., Mekori, Y. A., & Shefler, I. (2020). Lung cancer-derived extracellular vesicles: a possible mediator of mast cell activation in the tumor microenvironment. *Cancer Immunology, Immunotherapy*, *69*(3), 373–381.

Schroeder, B. C., Kubisch, C., Stein, V., & Jentsch, T. J. (1998). Moderate loss of function of cyclic-amp-modulated kcnq2/kcnq3 k+ channels causes epilepsy. *Nature*, *396*(6712), 687–690.

Shin, M. H., Kim, J., Lim, S. A., Kim, J., Kim, S.-J., & Lee, K.-M. (2020a). Nk cell-based immunotherapies in cancer. *Immune network*, *20*(2).

Shin, M. H., Kim, J., Lim, S. A., Kim, J., Kim, S.-J., & Lee, K.-M. (2020b). Nk cell-based immunotherapies in cancer. *Immune network*, *20*(2).

Sica, A., Allavena, P., & Mantovani, A. (2008). Cancer related inflammation: the macrophage connection. *Cancer letters*, *267*(2), 204–215.

Singh, N. A., Westenskow, P., Charlier, C., Pappas, C., Leslie, J., Dillon, J., . . . Leppert, M. F. (2003). Kcnq2 and kcnq3 potassium channel genes in benign familial neonatal convulsions: expansion of the functional and mutation spectrum. *Brain*, *126*(12), 2726–2737.

Soltis, A. R., Dalgard, C. L., Pollard, H. B., & Wilkerson, M. D. (2020). Mutenricher: a flexible toolset for somatic mutation enrichment analysis of tumor whole genomes. *BMC bioinformatics*, *21*(1), 1–8.

Spella, M., Lilis, I., Pepe, M. A., Chen, Y., Armaka, M., Lamort, A.-S., . . . others (2019). Club cells form lung adenocarcinomas and maintain the alveoli of adult mice. *Elife*, *8*, e45571.

Surti, T. S., Huang, L., Jan, Y. N., Jan, L. Y., & Cooper, E. C. (2005). Identification by mass spectrometry and functional characterization of two phosphorylation sites of kcnq2/kcnq3 channels. *Proceedings of the National Academy of Sciences*, *102*(49), 17828–17833.

Sutherland, K. D., Proost, N., Brouns, I., Adriaensen, D., Song, J.-Y., & Berns, A. (2011). Cell of origin of small cell lung cancer: inactivation of trp53 and rb1 in distinct cell types of adult mouse lung. *Cancer cell*, *19*(6), 754–764.

Tate John, G., Sally, B., Jubb Harry, C., Zbyslaw, S., Beare David, M., Nidhi, B., . . . Elisabeth, D. (2018). Stefancsik ray, thompson sam l, wang shicai, ward sari, campbell peter j, forbes simon a. cosmic: the catalogue of somatic mutations in cancer. *Nucleic Acids Research*, *47*(D1), D941–D947.

Tiffany, H. L., Lautens, L. L., Gao, J.-L., Pease, J., Locati, M., Combadiere, C., . . . Murphy, P. M. (1997). Identification of ccr8: a human monocyte and thymus receptor for the cc chemokine i-309. *The Journal of experimental medicine*, *186*(1), 165–170.

Travis, W. D. (2002). Pathology of lung cancer. *Clinics in chest medicine*, *23*(1), 65–81.

Tsuji, T., Ficarro, S. B., & Jiang, W. (2006). Essential role of phosphorylation of mcm2 by cdc7/dbf4 in the initiation of dna replication in mammalian cells. *Molecular biology of the cell*, *17*(10), 4459–4472.

Uhrig, S., Ellermann, J., Walther, T., Burkhardt, P., Fröhlich, M., Hutter, B., ... others (2021). Accurate and efficient detection of gene fusions from rna sequencing data. *Genome research*, *31*(3), 448–460.

Van der Auwera, G. A., Carneiro, M. O., Hartl, C., Poplin, R., Del Angel, G., Levy-Moonshine, A., ... others (2013). From fastq data to high-confidence variant calls: the genome analysis toolkit best practices pipeline. *Current protocols in bioinformatics*, *43*(1), 11–10.

Vaupel, P., & Mayer, A. (2007). Hypoxia in cancer: significance and impact on clinical outcome. *Cancer and Metastasis Reviews*, *26*(2), 225–239.

Vermi, W., Soncini, M., Melocchi, L., Sozzani, S., & Facchetti, F. (2011). Plasmacytoid dendritic cells and cancer. *Journal of leukocyte biology*, *90*(4), 681–690.

References XXX

Villarreal, D. O., L'Huillier, A., Armington, S., Mottershead, C., Filippova, E. V., Coder, B. D., . . . Princiotta, M. F. (2018). Targeting ccr8 induces protective antitumor immunity and enhances vaccine-induced responses in colon cancer. *Cancer research*, *78*(18), 5340–5348.

Wang, B.-Y., Huang, J.-Y., Chen, H.-C., Lin, C.-H., Lin, S.-H., Hung, W.-H., & Cheng, Y.-F. (2020). The comparison between adenocarcinoma and squamous cell carcinoma in lung cancer patients. *Journal of cancer research and clinical oncology*, *146*(1), 43–52.

Wang, C.-Z., Yano, H., Nagashima, K., & Seino, S. (2000). The na+-driven cl-/hco3- exchanger: Cloning, tissue distribution, and functional characterization* 210. *Journal of Biological Chemistry*, *275*(45), 35486–35490.

Wang, L., Darling, J., Zhang, J.-S., Liu, W., Qian, J., Bostwick, D., ... others (2000). Loss of expression of the drr 1 gene at chromosomal segment 3p21. 1 in renal cell carcinoma. *Genes, Chromosomes and Cancer*, *27*(1), 1–10.

Wedepohl, S., Dernedde, J., Vahedi-Faridi, A., Tauber, R., Saenger, W., & Bulut, H. (2017). Reducing macro-and microheterogeneity of n-glycans enables the crystal structure of the lectin and egf-like domains of human l-selectin to be solved at 1.9 å resolution. *ChemBioChem*, *18*(13), 1338–1345.

Wu, Z., Fournel, L., Stadler, N., Liu, J., Boullier, A., Hoyeau, N., ... others (2019). Modulation of lung cancer cell plasticity and heterogeneity with the restoration of cisplatin sensitivity by neurotensin antibody. *Cancer letters*, *444*, 147–161.

Wyles, J. P., Wu, Z., Mirski, S. E., & Cole, S. P. (2007). Nuclear interactions of topoisomerase ii α and β with phospholipid scramblase 1. *Nucleic acids research*, *35*(12), 4076–4085.

Xia, H.-W., Zhang, Z.-Q., Yuan, J., & Niu, Q.-L. (2021). Human recql5 promotes metastasis and resistance to cisplatin in non-small cell lung cancer. *Life Sciences*, *265*, 118768.

Xiao, H., He, M., Xie, G., Liu, Y., Zhao, Y., Ye, X., . . . Zhang, M. (2019). The release of tryptase from mast cells promote tumor cell metastasis via exosomes. *BMC cancer*, *19*(1), 1–9.

Ye, T., Yang, X., Liu, H., Lv, P., & Ye, Z. (2020). Long non-coding rna blacat1 in human cancers. *OncoTargets and therapy*, *13*, 8263.

Yin, J., Kwon, Y. T., Varshavsky, A., & Wang, W. (2004). Recql4, mutated in the rothmund–thomson and rapadilino syndromes, interacts with ubiquitin ligases ubr1 and ubr2 of the n-end rule pathway. *Human molecular genetics*, *13*(20), 2421–2430.

References XXXIII

Zeng, S., Liu, A., Dai, L., Yu, X., Zhang, Z., Xiong, Q., . . . others (2019). Prognostic value of top2a in bladder urothelial carcinoma and potential molecular mechanisms. *BMC cancer*, *19*(1), 1–12.

Zhang, J., Shao, J., Zhu, L., Zhao, R., Xing, J., Wang, J., . . . Yu, K. (2017). Molecular profiling identifies prognostic markers of stage ia lung adenocarcinoma. *Oncotarget*, *8*(43), 74846.

Zhu, T.-T., Sun, R.-L., Yin, Y.-L., Quan, J.-P., Song, P., Xu, J., . . . Li, P. (2019). Long noncoding rna uca1 promotes the proliferation of hypoxic human pulmonary artery smooth muscle cells. *Pflügers Archiv-European Journal of Physiology*, *471*(2), 347–355.

Zhu, X., Chen, H., Yang, Y., Xu, C., Zhou, J., Zhou, J., & Chen, Y. (2018). Distinct prognosis of mrna expression of the five recq dna-helicase family members–recql, blm, wrn, recql4, and recql5–in patients with breast cancer. *Cancer management and research*, *10*, 6649.